

Graph-based regularization for regression problems with highly-correlated designs

Yuan Li*, Garvesh Raskutti* and Rebecca Willett†

Abstract:

Sparse models for high-dimensional linear regression and machine learning have received substantial attention over the past two decades. Model selection, or determining which features or covariates are the best explanatory variables, is critical to the interpretability of a learned model. Much of the current literature assumes that covariates are only mildly correlated. However, in modern applications ranging from functional MRI to genome-wide association studies, covariates are highly correlated and do not exhibit key properties (such as the restricted eigenvalue condition, RIP, or other related assumptions). This paper considers a high-dimensional regression setting in which a graph governs both correlations among the covariates and the similarity among regression coefficients. Using side information about the strength of correlations among features, we form a graph with edge weights corresponding to pairwise covariances. This graph is used to define a graph total variation regularizer that promotes similar weights for highly correlated features. The graph structure encapsulated by this regularizer helps precondition correlated features to yield provably accurate estimates. Graph-based similarity measures have led to successful regularization in the cases of the fused LASSO, edge LASSO, and graph trend filtering; however, using graph-based regularizers to develop theoretical guarantees for highly-correlated covariates has not been previously examined. This paper shows how our proposed graph-based regularization yields mean-squared error guarantees for a broad range of covariance graph structures and correlation strengths which in many cases are optimal by imposing additional structure on β^* which encourages *alignment* with the covariance graph. Our proposed approach outperforms other state-of-the-art methods for highly-correlated design in a variety of experiments on simulated and real fMRI data.

1. Introduction

High-dimensional linear regression and inverse problems have received substantial attention over the past two decades (*cf.*, [Hastie, Tibshirani and Wainwright \(2015\)](#) for an overview). While there has been considerable theoretical and methodological development, applying these methods in real-world settings is more nuanced since variables or features are often highly correlated, while much of the existing theory and methodology is applicable when features are independent or satisfy weak correlation assumptions such as the restricted eigenvalue and other related conditions (*cf.*, [Bickel, Ritov and Tsybakov \(2009\)](#); [van de Geer and Bühlmann \(2009\)](#)). In this paper we develop an approach for parameter estimation in high-dimensional linear regression with highly-correlated designs.

More specifically, we consider observations of the form

$$y = X\beta^* + \epsilon \tag{1}$$

where $y \in \mathbb{R}^n$ is the response variable, $X \in \mathbb{R}^{n \times p}$ is the observation or *design* matrix, and $\epsilon \sim \mathcal{N}(\mathbf{0}, \sigma^2 I_{n \times n})$ is Gaussian noise. Our goal is to estimate β^* based on (X, y) when X potentially has highly-correlated columns and does not satisfy standard regularity assumptions. We consider the Gaussian linear model since it is more amenable to analysis but believe the ideas and results can be extended.

Highly-correlated or dependent features arise in many modern scientific problems. Consider, for instance, neural decoding using functional magnetic resonance imaging (fMRI) data. In this setting, we collect n

*Department of Statistics, University of Wisconsin-Madison. Raskutti and Li were supported by NSF DMS 1407028.

†Department of Electrical and Computer Engineering, University of Wisconsin-Madison. Willett was supported by NIH Award 1 U54 AI117924-01 and NSF Award 1740707.

different scans of a patient and let y_i indicate which stimulus was presented to the patient during the i^{th} scan for $i = 1, \dots, n$. The scan data is stored in X , with each row of X corresponding to a different fMRI scan and each column corresponding to a different voxel (small localized region of the brain). Each design matrix element $X_{i,j}$ would represent a statistic of the blood-oxygen-level dependent (BOLD) signal in the j^{th} voxel during the i^{th} scan (cf., Michel et al. (2011)). The model in (1) reflects that information about the stimulus is represented (or encoded) by voxels in the brain corresponding to the support of β^* . Because of the cost of fMRI experiments, it is typical to see on the order of one hundred scans and on the order of ten thousand voxels, resulting in a system that is under-determined by a factor of one hundred. In Section 5, we address a specific example involving fMRI. Similar challenges arise in genomics, such as genome-wide association studies (GWAS), where each column of X corresponds to a different single nucleotide polymorphism (SNP) and each row corresponds to a different subject's particular SNP realizations. In this application, the response variable y reflects each patient's disease state, and the goal is to determine which SNPs are potentially linked with a given disease (cf., Wu et al. (2009)). Again, the resulting system is typically underdetermined by a factor of about one hundred. In both settings, highly-correlated columns are unavoidable.

The key challenge associated with highly-correlated columns is that estimates of β^* become very sensitive to noise and, if columns are perfectly correlated, β^* may not be identifiable. For instance, if two voxels in the brain respond similarly to a stimulus in repeated trials, it becomes impossible to reliably determine which of the two voxels is potentially encoding information about the stimulus or if both are. Applying the classical LASSO (Tibshirani, 1996) estimator to such data would result in selecting the one voxel that is marginally more aligned with the stimulus. (That is, letting X_j denote the j^{th} column of X , if X_j is highly correlated with X_k , then the LASSO would choose β_j to be nonzero and β_k to be zero valued when $\langle X_j, y \rangle > \langle X_k, y \rangle$; this test has low power and is sensitive to noise.)

1.1. Problem formulation and proposed estimator

First we define our model based on the standard linear model where data $(X^{(i)}, y^{(i)})_{i=1}^n \in \mathbb{R}^p \times \mathbb{R}$ are drawn i.i.d. according to

$$y^{(i)} = X^{(i)\top} \beta^* + \epsilon^{(i)}, \text{ where } X^{(i)} \sim \mathcal{N}(\mathbf{0}, \Sigma_{p \times p}) \text{ and } \epsilon^{(i)} \sim \mathcal{N}(0, \sigma^2).$$

Let $y = (y^{(1)}, y^{(2)}, \dots, y^{(n)})^\top \in \mathbb{R}^n$, $X = [X^{(1)}, X^{(2)}, \dots, X^{(n)}]^\top \in \mathbb{R}^{n \times p}$ and $\epsilon = (\epsilon^{(1)}, \epsilon^{(2)}, \dots, \epsilon^{(n)})^\top \in \mathbb{R}^n$. Hence the linear model can be expressed in the standard matrix-vector form:

$$y = X\beta^* + \epsilon.$$

Our goal is to estimate β^* .

We assume Σ is unknown and is estimated using either X or side information; let $\hat{\Sigma}$ denote the estimate of the covariance matrix. Define $\hat{s}_{j,k} := \text{sign}(\hat{\Sigma}_{j,k})$. Based on the estimated covariance matrix $\hat{\Sigma}$, we consider the following estimator for β^* :

$$\begin{aligned} \hat{\beta} = \arg \min_{\beta} & \frac{1}{n} \|y - X\beta\|_2^2 + \lambda_S \sum_{j,k} |\hat{\Sigma}_{j,k}| (\beta_j - \hat{s}_{j,k} \beta_k)^2 \\ & + \lambda_1 (\lambda_{\text{TV}} \sum_{j,k} |\hat{\Sigma}_{j,k}|^{1/2} |\beta_j - \hat{s}_{j,k} \beta_k| + \|\beta\|_1), \end{aligned} \quad (2)$$

where λ_S , λ_1 and λ_{TV} are regularization parameters.

This estimator can be interpreted from a graph/network perspective by defining the *covariance graph* based on the covariance matrix $\hat{\Sigma}$. Let $G = (V, E, W)$ be an undirected weighted graph where $V =$

$\{1, 2, \dots, p\}$ with edge weight $w_{j,k}$ ($1 \leq j \neq k \leq p$) associated with edge $(j, k) \in E$. The edge weights corresponding to $W = (w_{j,k})$ may be negative. Now we define our covariance graph. Let $w_{j,k} = \hat{\Sigma}_{j,k}$, which denotes the (j, k) entry of the covariance matrix $\hat{\Sigma}$. Then $E := \{(j, k) : w_{j,k} \neq 0, j \neq k\}$ and the entries of the weight matrix $W \in \mathbb{R}^{p \times p}$ are $W_{j,k} = w_{j,k}$. Given this graph, the regularization term $\sum_{j,k} |\hat{\Sigma}_{j,k}|^{1/2} |\beta_j - \hat{s}_{j,k} \beta_k|$ is a measure of the *graph total variation* of the signal β with respect to the graph G and $\sum_{j,k} |\hat{\Sigma}_{j,k}| (\beta_j - \hat{s}_{j,k} \beta_k)^2$ corresponds to a *graph Laplacian regularizer* with respect to G .

Further let Γ be the *weighted edge incidence matrix* associated with the graph G . Specifically, we denote the set of edges in our graph as (j_ℓ, k_ℓ) for $\ell = 1, \dots, m$ where $m := |E|$ is the size of the edge set. Let

$$\Gamma = \sum_{\ell=1}^m \Gamma_\ell, \quad \text{where} \quad \Gamma_\ell := |\hat{\Sigma}_{j_\ell, k_\ell}|^{1/2} u_\ell \left[e_{j_\ell} - \text{sign}(\hat{\Sigma}_{j_\ell, k_\ell}) e_{k_\ell} \right]^\top \in \mathbb{R}^{m \times p}, \quad (3)$$

where $u_\ell \in \mathbb{R}^m$ and $e_\ell \in \mathbb{R}^p$ are the ℓ^{th} canonical basis vectors (all zeros except for a one in the ℓ^{th} element). Then the ℓ^{th} row of Γ is

$$|\hat{\Sigma}_{j_\ell, k_\ell}|^{1/2} \left[e_{j_\ell} - \text{sign}(\hat{\Sigma}_{j_\ell, k_\ell}) e_{k_\ell} \right]^\top.$$

Next suppose $\lambda_1 > 0$ and $\lambda_{TV}, \lambda_S \geq 0$. We define

$$\tilde{X} = \tilde{X}_{\lambda_S} := \left[\frac{X}{\sqrt{n\lambda_S}\Gamma} \right] \in \mathbb{R}^{(n+m) \times p}, \quad \tilde{y} := \begin{bmatrix} y \\ \mathbf{0}_{m \times 1} \end{bmatrix} \in \mathbb{R}^{n+m}, \quad \text{and} \quad \tilde{\Gamma} := \begin{bmatrix} \lambda_{TV}\Gamma \\ I_{p \times p} \end{bmatrix} \in \mathbb{R}^{(m+p) \times p}.$$

Using these definitions, we may write the estimator (2) equivalently as

$$\hat{\beta} = \arg \min_{\beta} \frac{1}{n} \|y - X\beta\|_2^2 + \lambda_S \|\Gamma\beta\|_2^2 + \lambda_1 (\lambda_{TV} \|\Gamma\beta\|_1 + \|\beta\|_1) \quad (4)$$

$$= \arg \min_{\beta} \frac{1}{n} \|\tilde{y} - \tilde{X}\beta\|_2^2 + \lambda_1 \|\tilde{\Gamma}\beta\|_1. \quad (5)$$

The three regularizers play the following roles:

- We refer to $\|\Gamma\beta\|_2^2 = \sum_{j,k} |\hat{\Sigma}_{j,k}| (\beta_j - \hat{s}_{j,k} \beta_k)^2$ as the **Laplacian smoothing penalty**; [Hebiri and van de Geer \(2011\)](#) studied a variant of this regularizer with $\hat{\Sigma}_{j,k}$ replaced with arbitrary non-negative weights. Because each term is squared, it helps to reduce the ill-conditionedness of X when columns are highly correlated, as reflected in our analysis.
- We refer to $\|\Gamma\beta\|_1 = \sum_{j,k} |\hat{\Sigma}_{j,k}|^{1/2} |\beta_j - \hat{s}_{j,k} \beta_k|$ as the **total variation penalty**, as do [Shuman et al. \(2013\)](#); [Wang et al. \(2016\)](#); [Sadhanala, Wang and Tibshirani \(2016\)](#); [Hütter and Rigollet \(2016\)](#); it is closely related to the edge LASSO penalty ([Sharpnack, Singh and Rinaldo, 2012](#)). Note that these prior works consider general weighted graphs (instead of graphs defined by a covariance matrix $\hat{\Sigma}$, as we do). This regularizer promotes estimates $\hat{\beta}$ that are *well-aligned* with the graph structure; for instance, a group of nodes with large edge weights connecting them (*i.e.*, a group of columns of X that are highly correlated) are more likely to be associated with coefficient estimates with similar values.
- We refer to $\|\beta\|_1$ as the **sparsity regularizer**. The combination of the sparsity regularizer and total variation penalty amount to the fused LASSO ([Tibshirani et al., 2005](#); [Tibshirani and Taylor, 2011](#)).

The combined effect of the three regularization terms is to find estimates of β^* which are both a good fit to the data when the columns of X are highly correlated and well-aligned with the underlying graph.

1.2. Contributions

This paper addresses the question of how to estimate β^* from observations in (1) when X has highly-correlated columns. We propose a regularized regression approach in which the regularization function depends upon the covariance of X . For a fixed graph G , the proposed estimator is closely related to the previously-proposed fused LASSO (Tibshirani et al., 2005), generalized LASSO (Tibshirani and Taylor, 2011), edge LASSO (Sharpnack, Singh and Rinaldo, 2012), network LASSO (Hallac, Leskovec and Boyd, 2015), trend filtering (Wang et al., 2016), and total-variation regularization (Shuman et al., 2013; Hütter and Rigollet, 2016). In contrast to these past efforts, our focus is on settings in which columns of X are highly correlated and these correlations inform the choice of graph G .

On the other hand there is a large body of work on highly dependent features; in Section 2 we provide a thorough comparison of our method with other related approaches. In this paper we make the following novel contributions:

- A novel estimator with corresponding finite-sample theoretical guarantees for highly-correlated design matrices X . General theoretical guarantees provide novel insight into the impact of the alignment of β^* with the covariance graph, and properties of the covariance graph structure such as smallest and largest block-sizes and smallest non-zero eigenvalue.
- New guarantees for two specific covariance graph structures, a block complete graph and a chain graph. Our mean-squared error bounds match the optimal rates in the independent case, and also match previous error bounds (Figueiredo and Nowak, 2016) for the block complete covariance graph.
- A simulation study which shows that our method out-performs state-of-the-art alternatives such as the Cluster Representative LASSO (CRL, Bühlmann et al. (2013)) and Ordered Weighted LASSO (OWL, Figueiredo and Nowak (2016)) in terms of mean squared error.
- A validation of our method on real fMRI data that demonstrates that our method out-performs state-of-the-art methods in terms of prediction error.

The remainder of this paper is organized as follows: In Section 2 we discuss existing work and results for this problem and its relationship to our estimator; in Section 3 we present our main theoretical results; in Section 4 we carry out a simulation study by comparing our methods to other state-of-the-art methods; in Section 5 we apply our method to a real fMRI dataset with comparison to other methods; proofs are provided in Sections 6 and Section 8; we state our conclusions in Section 7.

2. Relationship to prior work

As mentioned earlier, variants of the proposed estimator have been widely studied in past works. We review these past works below.

2.1. Prior work: “Denoising” settings

Significant effort has been devoted to understanding estimators like (4) in the special case where $X = I$ – that is, in a “denoising” setting in which observations are direct measurements of the signal of interest, β . Variants of these estimators are often referred to as the edge or network LASSO (Sharpnack, Singh and Rinaldo, 2012; Hallac, Leskovec and Boyd, 2015), a special case of graph trend filtering (Wang et al., 2016), or graph total variation estimation (Shuman et al., 2013). In these settings, we assume a known graph or network $G = (V, E)$, where each edge connecting nodes $v_j \in V$ and $v_k \in V$ is associated with a non-negative edge weight $w_{j,k}$. Zero-valued edge weights are equivalent to the absence of an edge. The edge

LASSO estimator or graph trend filter has the form

$$\hat{\beta} = \arg \min_{\beta} \frac{1}{n} \|y - \beta\|_2^2 + \lambda_{\text{TV}} \sum_{1 \leq j < k \leq n} w_{j,k} |\beta_j - \beta_k|.$$

In particular, [Sharpnack, Singh and Rinaldo \(2012\)](#) assume a known underlying graph and that the true generating parameter β^* is piece-wise constant over an unknown partition of the vertices and study the “sparsistency” of the edge LASSO estimator – essentially, the conditions under which the edge LASSO estimate and the generating β^* are supported on the same graph partition. [Hallac, Leskovec and Boyd \(2015\)](#) describe a “network LASSO” problem and propose a scalable Alternating Direction Method of Multipliers (ADMM) algorithm that can be implemented on distributed computers and guarantees global convergence even on large graphs.

The above ideas are also closely related to work on “graph signal processing” ([Shuman et al. \(2013\)](#) provide an excellent overview), in which classical concepts of frequency domain representations of signals, filtering, translation, and modulation are all generalized to signals observed on the vertices of graphs. In particular, the regularization function $\sum_{1 \leq j < k \leq n} w_{j,k} |\beta_j - \beta_k|$ is referred to as the *total variation* of the signal with respect to the graph.

[Wang et al. \(2016\)](#) consider a generalization of graph total variation to higher-order measures of variation of signals for denoising piecewise-polynomial signals on graphs and derive squared error bounds for the estimates. Those bounds do not account for a sensing matrix X other than $X = I$. [Hütter and Rigollet \(2016\)](#) also develop sharp oracle inequalities for the edge LASSO, with an emphasis on a 2d lattice graph used in image processing applications.

2.2. Prior work: Regression/inverse problem settings

The original work on the *fused LASSO* ([Tibshirani et al., 2005](#)) considers estimators of the form

$$\hat{\beta} = \arg \min_{\beta} \frac{1}{n} \|y - X\beta\|_2^2 + \lambda_{\text{TV}} \sum_{j=1}^{p-1} |\beta_j - \beta_{j+1}| + \lambda_1 \|\beta\|_1.$$

Their theory yielded asymptotic properties for fixed p and $n \rightarrow \infty$. The *generalized LASSO* of [Tibshirani and Taylor \(2011\)](#); [Liu, Yuan and Ye \(2013\)](#) consider the estimators of the form

$$\hat{\beta} = \arg \min_{\beta} \frac{1}{n} \|y - X\beta\|_2^2 + \lambda \|\Gamma\beta\|_1 \tag{6}$$

for general X and Γ ; note that both the fused LASSO and the estimator in (4) can be written in this form. [Tibshirani and Taylor \(2011\)](#) consider the solution path of this estimator, a variety of optimization and computational considerations, and a degrees-of-freedom analysis. Understanding the degrees-of-freedom of an estimator is a crucial step towards sample complexity bounds emphasized in this paper, but the past work does not consider the role of correlations among columns of X relative to the choice of regularizer and the subsequent impact on performance. In particular, their analysis focuses on the setting in which $\text{rank}(X) = p$, a condition we do not assume in our setting. Related work by [Needell and Ward \(2013a,b\)](#) consider the special case of the generalized LASSO of total variation regularization on a grid for image reconstruction problems. That analysis, while elegant, relies heavily upon the grid-like graph structure associated with pixels in images and does not generalize to the setting of this paper. In addition, they assume that the design matrix X satisfies the *restricted isometry property* ([Candes and Tao, 2005](#)), a condition similar to

the restricted eigenvalue condition described below that is generally not met when columns of X are highly correlated.

Estimators similar to (4) have been explored empirically in a variety of application settings; (cf., [Grosenick et al. \(2009\)](#); [Michel et al. \(2011\)](#); [Grosenick et al. \(2011\)](#); [Shen, Huang and Pan \(2012\)](#); [Xin et al. \(2014, 2016\)](#); [Jalali and Fazel \(2013\)](#)). However, these studies are mainly empirical and do not provide performance guarantees that are the focus of this paper.

2.3. Prior work: Highly correlated design matrices

A key focus of our work is the setting in which columns of X may be highly correlated. Correlated columns arise frequently in applications, as discussed in the introduction. There are several approaches developed to deal with the high-dimensional linear regression problem with some highly correlated covariates. The *Elastic Net* estimator proposed by [Zou and Hastie \(2005\)](#) is

$$\hat{\beta} = \arg \min_{\beta} \|y - X\beta\|_2^2 + \lambda_1 \|\beta\|_1 + \lambda_S \|\beta\|_2^2, \quad (7)$$

which encourages a grouping effect, in which strongly-correlated predictors tend to be in or out of the support of the estimate together. [Witten, Shojaie and Zhang \(2014\)](#) propose a *Cluster Elastic Net* estimator:

$$\hat{\beta} = \arg \min_{\beta} \|y - X\beta\|_2^2 + \lambda_1 \|\beta\|_1 + \lambda_S \sum_{k=1}^K \frac{1}{|C_k|} \sum_{i,j \in C_k} \|X_i \beta_i - X_j \beta_j\|_2^2,$$

where C_1, \dots, C_k denotes a fixed partition of the p features into K groups. This estimator incorporates clustering information inferred from data to perform more accurate regression.

An alternative approach explored by [Bühlmann et al. \(2013\)](#), called *Cluster Representative LASSO (CRL)*, clusters highly correlated columns of X , chooses a single representative for each cluster, and regresses over the cluster centers. In our fMRI example from above, the two correlated voxels would be clustered together, and the resulting CRL estimate would indicate simply that one or more members of the clusters are good predictors of the stimulus. [Bühlmann et al. \(2013\)](#) also considered a *Cluster Group LASSO (CGL)* in which a group sparsity regularizer was used with the original design matrix X and the group structure was determined by a clustering of the columns of X . These two-stage approaches (first cluster, then regress based on estimated clusters) admitted encouraging statistical guarantees and empirical performance. However, (i) they depend heavily upon our ability to find a good clustering of the columns of X , where clusters must be disjoint or non-overlapping; (ii) clustering decisions are “hard” and do not reflect varying degrees of correlation among columns, and (iii) clusters are formed independently of the observed responses (y). Constraint (i) is particularly challenging to meet in real-world applications, including our motivating application of fMRI. If we wish to force non-overlapping clusters, then there is potentially more than one “good” candidate clustering of the data; in this case, y can potentially provide valuable insight into which candidate clustering is most relevant to the regression task, but the CRL and CGL estimators do not leverage y in the clustering phase and it is not immediately clear how one would make this extension. *Grouping pursuit* ([Shen and Huang, 2010](#)) explores clustering columns of X while leveraging y by using a non-convex variant of the fused LASSO.

Other approaches sidestep explicit estimation of correlations among columns of X . Early work on the adaptive LASSO by [Zou \(2006\)](#) illustrated the impact of adaptivity in the correlated design setting. Recent work on the *Ordered Weighted LASSO (OWL)* estimator ([Figueiredo and Nowak, 2016](#)) proposed an alter-

native weighted LASSO regularizer in which the weights depend on the order statistics of β ; specifically,

$$\hat{\beta} = \arg \min_{\beta} \|y - X\beta\|_2^2 + \lambda_1 \sum_{j=1}^p w_j |\beta|_{[j]},$$

where $w_1 \geq w_2 \geq \dots \geq w_p \geq 0$ and $|\beta|_{[j]}$ is the j^{th} largest element in $\{|\beta_1|, |\beta_2|, \dots, |\beta_p|\}$, their paper shows that this family of regularizers can be used for sparse linear regression with strongly correlated covariates.

A special case of OWL is the *OSCAR* estimator (Bondell and Reich, 2008), which takes the form

$$\hat{\beta} = \arg \min_{\beta} \frac{1}{n} \|y - X\beta\|_2^2 + \lambda_{\text{TV}} \sum_{1 \leq j < k \leq p} |\beta_j| \vee |\beta_k| + \lambda_1 \|\beta\|_1.$$

Figueiredo and Nowak (2016) demonstrated that when two columns of X were *identical*, then OWL would assign the corresponding elements of β equal values. OWL adaptively groups highly correlated columns of X by assigning them equal weights whenever their correlation exceeds a critical value – the grouping does not need to be pre-computed and will depend on the value of y . However, we still do not fully understand the performance of the OWL for design matrices with more moderately correlated columns. Finally, unlike the CRL, CGL, and the proposed GTV estimator (4), the OWL has no mechanism for incorporating possible side information about the correlation among different columns of X .

A related approach is the *clustered LASSO* (She, 2010), which takes the form

$$\hat{\beta} = \arg \min_{\beta} \frac{1}{n} \|y - X\beta\|_2^2 + \lambda_{\text{TV}} \sum_{1 \leq j < k \leq p} |\beta_j - \beta_k| + \lambda_1 \|\beta\|_1.$$

In contrast to the fused LASSO, the clustered LASSO considers *all* pairwise differences of elements of β . She (2010) conducts a classical asymptotic analysis (fixed p and $n \rightarrow \infty$) of the clustered LASSO and its generalization (6) and establishes consistency results that depend upon Σ^{-1} ; note that Σ will have very small singular values when columns of X are highly correlated. A similar estimator called *Pairwise Absolute Clustering and Sparsity (PACS)* estimator is proposed by Sharma, Bondell and Zhang (2013):

$$\hat{\beta} = \arg \min_{\beta} \frac{1}{n} \|y - X\beta\|_2^2 + \lambda_1 \left\{ \sum_{j=1}^p w_j |\beta_j| + \sum_{1 \leq j < k \leq p} w_{jk(-)} |\beta_k - \beta_j| + \sum_{1 \leq j < k \leq p} w_{jk(+)} |\beta_k + \beta_j| \right\},$$

where the w_j s, $w_{jk(-)}$ s and $w_{jk(+)}$ s are non-negative weights chosen in penalization scheme. This PACS estimator depends heavily on the choice of non-negative weights. One suggestion offered by Sharma, Bondell and Zhang (2013) in the setting of correlated variables is $w_j = 1$, $w_{jk(-)} = \sqrt{2(1 - r_{jk})}$ and $w_{jk(+)} = \sqrt{2(1 + r_{jk})}$ for $1 \leq j < k \leq p$, where r_{jk} is the correlation between (j, k) th pair of covariates. Hebiri and van de Geer (2011) consider smooth *S-LASSO* estimators of the form

$$\hat{\beta} = \arg \min_{\beta} \frac{1}{n} \|y - X\beta\|_2^2 + \lambda_S \|\Gamma\beta\|_2^2 + \lambda_1 \|\beta\|_1.$$

The first regularization term, unlike the total variation term in (4), is a quadratic penalty similar to what appears in the elastic net (7) (Zou and Hastie, 2005). The analyses by She (2010), Sharma, Bondell and Zhang (2013) and Hebiri and van de Geer (2011) do not consider settings in which X and Γ in (6) are related. Dayer and Jeng (2009) propose a *weighted fusion estimator*,

$$\hat{\beta} = \arg \min_{\beta} \|y - X\beta\|_2^2 + \frac{\lambda_S}{p} \sum_{1 \leq j < k \leq p} w_{jk} (\beta_j - s_{jk} \beta_k)^2 + \lambda_1 \|\beta\|_1,$$

where $s_{jk} = \text{sign}(X_j^T X_k)$ and $w_{jk} \propto |X_j^T X_k|$; this approach is similar to [Hebiri and van de Geer \(2011\)](#) for a particular choice of weights. [Daye and Jeng \(2009\)](#) focus their analysis on grouping effects, sign consistency, and limiting distributions, but do not consider finite sample error bounds of the type developed in this paper. The *Sparse Laplacian Shrinkage (SLS)* estimator proposed by [Huang et al. \(2011\)](#) uses a *minimum concave penalty (MCP)* to replace the LASSO penalty in a weighted fusion estimator to reduce bias; specifically, the SLS estimator has the following form:

$$\hat{\beta} = \arg \min_{\beta} \frac{1}{n} \|y - X\beta\|_2^2 + \sum_{j=1}^p \rho(|\beta_j|; \lambda_1, \gamma) + \lambda_S \sum_{1 \leq i < j \leq p} w_{jk} (\beta_j - s_{jk} \beta_k)^2,$$

where ρ is the MCP with penalty parameter λ_1 and regularization parameter γ , the definitions of w_{jk} and s_{jk} are the same with weighted fusion estimator. [Huang et al. \(2011\)](#) provide analysis for sign consistency and selection properties of SLS estimator, but no finite sample error results are provided.

3. Assumptions and Main Results

In this section, we first introduce the assumptions for our main results. Throughout we use the induced matrix norm notation

$$\|A\|_{p,q} = \sup_{x \neq 0} \frac{\|Ax\|_q}{\|x\|_p}.$$

Specifically, note that $\|A\|_{1,2}$ is the maximum column norm of A and $\|A\|_{op} = \|A\|_{2,2}$. Further for a symmetric positive semi-definite matrix A , let $\lambda_{\min}(A)$ denote its minimum eigenvalue and $\lambda_{\max}(A)$ denote its maximum eigenvalue.

The notation $X_n = O_P(a_n)$ means that the set of values $\frac{X_n}{a_n}$ is stochastically bounded. That is, for any $\epsilon > 0$, there exists a finite $M > 0$ and a finite $N > 0$ such that

$$\mathbb{P} \left(\left| \frac{X_n}{a_n} \right| > M \right) < \epsilon, \forall n > N.$$

Assumption 3.1. We assume that there exists an absolute constant $c_u > 0$ such that

$$\lambda_{\max}(\Sigma) \leq c_u.$$

Remark 3.1. This statement assumes that Σ is normalized such that the largest eigenvalue of Σ can be upper bounded by a positive constant.

Assumption 3.2. There exists an absolute constant $c_\ell > 0$ such that:

$$c_\ell \leq \min_{1 \leq j \leq p} \sum_{k=1}^p |\Sigma_{j,k}|.$$

Remark 3.2. Assumption 3.2 ensures the ℓ_1 norm for each row/column is lower bounded by a constant. This assumption is much milder than assuming the minimum eigenvalue of Σ is bounded away from 0 and is satisfied for example in cases where every diagonal entry of Σ is bounded below by c_ℓ and many other cases.

Assumption 3.3. The estimated covariance matrix $\hat{\Sigma}$ that is used to construct matrix Γ satisfies

$$\|\hat{\Sigma} - \Sigma\|_{1,1} = \max_{1 \leq j \leq p} \sum_{k=1}^p |\hat{\Sigma}_{j,k} - \Sigma_{j,k}| \leq \frac{c_\ell}{4},$$

where c_ℓ is defined in Assumption 3.2.

Remark 3.3. Assumption 3.3 states that we need a sufficiently accurate estimator $\hat{\Sigma}$ for Σ . If Assumption 3.3 is satisfied then we can use $\hat{\Sigma}$ to construct Γ for our optimization problem stated in (5). In some cases, we estimate Σ using side information that is not based on $(X^{(i)})_{i=1}^n$. If we need to estimate Σ based on $(X^{(i)})_{i=1}^n$, there is a large literature on high-dimensional covariance estimation in high dimensions under different structural assumptions (cf., [Bickel and Levina \(2008a,b\)](#); [Cai and Liu \(2011\)](#); [Cai, Zhao and Zhou \(2016\)](#); [Donoho, Gavish and Johnstone \(2013\)](#); [Baik and Silverstein \(2006\)](#)). As an example, we consider estimators based on thresholding the sample covariance matrix under sparsity assumptions developed by [Bickel and Levina \(2008b\)](#).

To be specific, suppose the true covariance matrix Σ belongs to the following class:

$$\Omega(q, c_0(p), M) = \left\{ \Sigma : \Sigma_{j,j} \leq M, \sum_{k=1}^p |\Sigma_{j,k}|^q \leq c_0(p), \text{ for all } j \right\},$$

where $0 \leq q < 1$, $c_0(p)$ is a constant that depends on p and M is an absolute constant. Then [Bickel and Levina \(2008b\)](#), Theorem 1) show that if we define the thresholded covariance matrix $\hat{\Sigma}_{j,k} = S_{j,k} \mathbb{1}(|S_{j,k}| \geq t)$ for all $1 \leq j, k \leq p$ where S is the sample covariance matrix and $t = O\left(\sqrt{\frac{\log p}{n}}\right)$, then

$$\|\hat{\Sigma} - \Sigma\|_{1,1} = O_P\left(c_0(p)M \left(\frac{\log p}{n}\right)^{\frac{1-q}{2}}\right).$$

Though the original error bound result for $\hat{\Sigma} - \Sigma$ in [Bickel and Levina \(2008b\)](#) was shown in operator norm, they bounded $\|\hat{\Sigma} - \Sigma\|_{1,1}$ in the proof. In particular if $q = 0$ and $c_0(p) \leq s$ denotes the sparsity level,

$$\|\hat{\Sigma} - \Sigma\|_{1,1} = O_P\left(s\sqrt{\frac{\log p}{n}}\right),$$

meaning if $n = O(s^2 \log p)$, Assumption 3.3 is satisfied.

On the other hand, if the covariance matrix Σ is not sparse but block-structured, we can use an alternative bound developed in [Bickel and Levina \(2008b\)](#). In particular, if Σ has K identical blocks where each block has p/K elements, to ensure Assumptions 3.1 and 3.2 are satisfied $\Sigma_{j,k} = O\left(\frac{K}{p}\right)$ for each non-zero $\Sigma_{j,k}$. Then if we choose $\hat{\Sigma}$ to be the sample covariance matrix, [Bickel and Levina \(2008b\)](#) prove that

$$\max_{j,k} \left| \frac{\hat{\Sigma}_{j,k} - \Sigma_{j,k}}{K/p} \right| = O_P\left(\sqrt{\frac{\log p}{n}}\right) \quad (8)$$

since now we have $\frac{\Sigma_{j,j}}{K/p} = O(1)$ for $1 \leq j \leq p$. Thus by (8) we know that

$$\max_{j,k} |\hat{\Sigma}_{j,k} - \Sigma_{j,k}| = O_P\left(\frac{K}{p} \sqrt{\frac{\log p}{n}}\right) \quad (9)$$

and

$$\|\hat{\Sigma} - \Sigma\|_{1,1} = \max_{1 \leq j \leq p} \sum_{k=1}^p |\hat{\Sigma}_{j,k} - \Sigma_{j,k}| = O_P\left(K \sqrt{\frac{\log p}{n}}\right)$$

by (9), so that when $n = O(K^2 \log p)$ Assumption 3.3 is satisfied.

In addition to the above properties of the covariance matrix, the performance of our estimator depends upon the following two properties of the augmented edge incidence matrix $\tilde{\Gamma}$ appearing in our regularizer:

Definition 3.1 (Compatibility factor k_T , [Hütter and Rigollet \(2016\)](#)). We define the compatibility factor k_T of matrix $\tilde{\Gamma}$ for a set $T \subset \{1, 2, \dots, p, p+1, \dots, p+m\}$ as:

$$k_\emptyset := 1, \quad k_T := \inf_{\beta \in \mathbb{R}^p} \frac{\sqrt{|T|} \|\beta\|_2}{\|(\tilde{\Gamma}\beta)_T\|_1} \text{ for } T \neq \emptyset.$$

This compatibility factor k_T reflects the degree of compatibility of ℓ_1 -regularizer $\|(\tilde{\Gamma}\beta)_T\|_1$ and the ℓ_2 -error norm $\|\beta\|_2$ for a set T . This compatibility factor appears explicitly in the bounds of our main theorem.

Definition 3.2 (Inverse scaling factor ρ , [Hütter and Rigollet \(2016\)](#)). Let $S := \tilde{\Gamma}^\dagger = [s_1, \dots, s_{m+p}]$, where $\tilde{\Gamma}^\dagger$ is the Moore-Penrose pseudoinverse of matrix $\tilde{\Gamma}$, and define the inverse scaling factor as:

$$\rho := \|\tilde{\Gamma}^\dagger\|_{1,2} = \max_{j=1,2,\dots,m+p} \|s_j\|_2.$$

Remark 3.4. Definition 3.1 and 3.2 are first proposed in [Hütter and Rigollet \(2016\)](#), though the definition of ρ is based on $\tilde{\Gamma}$ rather than Γ , as discussed in Remark 3.9. Later we will see that ρ and k_T are crucial for our main results. Note that

$$\frac{\rho}{k_T} := \sup_{\beta \in \mathbb{R}^p, \beta \neq 0} \frac{\|(\tilde{\Gamma}\beta)_T\|_1 \|\tilde{\Gamma}^\dagger\|_{1,2}}{\sqrt{|T|} \|\beta\|_2} \leq \sup_{\beta \in \mathbb{R}^p, \beta \neq 0} \frac{\sqrt{|T|} \|\tilde{\Gamma}\beta\|_2 \|\tilde{\Gamma}^\dagger\|_{1,2}}{\sqrt{|T|} \|\beta\|_2} = \|\tilde{\Gamma}\|_{op} \|\tilde{\Gamma}^\dagger\|_{1,2}.$$

The quantity $\frac{\rho}{k_T}$ is similar in flavour to the condition number of the matrix $\tilde{\Gamma}$.

Finally, we define the *weighted graph Laplacian* $L := \Gamma^\top \Gamma$. Spectral properties of L , in particular block sizes and smallest non-zero eigenvalues in each block will play a crucial role in the mean-squared error bounds we derive. By the definition of Γ , it follows that

$$L = \begin{bmatrix} \sum_{k=2}^p |\hat{\Sigma}_{1,k}| & -\hat{\Sigma}_{1,2} & -\hat{\Sigma}_{1,3} & \cdots & -\hat{\Sigma}_{1,p} \\ -\hat{\Sigma}_{2,1} & \sum_{i=1, i \neq 2}^p |\hat{\Sigma}_{2,i}| & -\hat{\Sigma}_{2,3} & \cdots & -\hat{\Sigma}_{2,p} \\ \cdots & \cdots & \cdots & \cdots & \cdots \\ -\hat{\Sigma}_{p,1} & -\hat{\Sigma}_{p,2} & -\hat{\Sigma}_{p,3} & \cdots & \sum_{k=1}^{p-1} |\hat{\Sigma}_{p,k}| \end{bmatrix}_{p \times p}.$$

Theorem 1. Suppose $\lambda_1 > 0$ and Assumptions 3.1 to 3.3 are satisfied. If

$$\lambda_1 \geq \max \left\{ 48\rho\sigma \sqrt{\frac{c_u \log p}{n}}, 8\lambda_S \|L\beta^*\|_\infty \right\},$$

then there exist absolute positive constants C_u and C_1 such that with probability at least $1 - \frac{C_1}{p}$ we have

$$\|\hat{\beta} - \beta^*\|_2^2 \leq C_u \min_T \max \left\{ \frac{\lambda_1^2 |T|}{k_T^2 \lambda_{\min}^2 (\Sigma + \lambda_S L)}, \frac{\lambda_1 \|(\tilde{\Gamma}\beta^*)_{T^c}\|_1 + \lambda_1^2 \|(\tilde{\Gamma}\beta^*)_{T^c}\|_1^2}{\lambda_{\min} (\Sigma + \lambda_S L)} \right\}$$

provided $\frac{\lambda_1^2 |T|}{k_T^2 \lambda_{\min}^2 (\Sigma + \lambda_S L)} \rightarrow 0$ (i.e., that the estimator is consistent).

Remark 3.5. Here $\lambda_{\min}(\Sigma + \lambda_S L)$ plays the role of the restricted eigenvalue constant (see [Bickel, Ritov and Tsybakov \(2009\)](#) for more details about this condition). Recall that from the definition of L , if we define the diagonal matrix $D \in \mathbb{R}^{p \times p}$ where each diagonal entry is $D_{jj} = \sum_{k=1}^p |\hat{\Sigma}_{j,k}|$, $1 \leq j \leq p$, then it follows that

$$\Sigma + L := \Sigma - \hat{\Sigma} + D.$$

Hence if Σ and $\hat{\Sigma}$ are “close” as is specified by Assumption 3.3, then $\Sigma + L$ is “close” to a diagonal matrix which ensures that $\lambda_{\min}(\Sigma + \lambda_S L)$ may be bounded away from 0, even if $\lambda_{\min}(\Sigma) = 0$. The following Lemma makes this statement precise:

Lemma 1. *Suppose that Assumption 3.2 and 3.3 are satisfied and $0 \leq \lambda_S \leq 1$. Then*

$$\lambda_{\min}(\Sigma + \lambda_S L) \geq (1 - \lambda_S) \lambda_{\min}(\Sigma) + \lambda_S \frac{c_\ell}{2}.$$

The proof is deferred to the appendix. Thus even if $\lambda_{\min}(\Sigma) = 0$, choosing λ_S bounded away from 0 results in a well-posed inverse problem. On the other hand, in the classical LASSO analysis where $\lambda_{\min}(\Sigma) > 0$, we can choose $\lambda_S = 0$.

Remark 3.6. $\|L\beta^*\|_\infty$ can be seen as a measure of the *misalignment* of the signal β^* and the graph represented by the matrix Γ . Note that we require $\lambda_1 \geq 8\lambda_S \|L\beta^*\|_\infty$. Hence there is a clear trade-off in the choice of λ_S . Choosing λ_S close to 1 ensures $\lambda_{\min}(\Sigma + \lambda_S L)$ is bounded away from 0 but incurs a cost that scales with $\|L\beta^*\|_\infty$.

In general, if $\lambda_{\min}(\Sigma) = 0$, indicating high correlations, we require $\|L\beta^*\|_\infty \approx 0$ (i.e., β^* is well-aligned with L) in order to obtain consistent mean-squared error bounds. Note that analysis of OWL ([Figueiredo and Nowak, 2016](#)) assumes $L\beta^* = \mathbf{0}$ (perfect alignment). If $\lambda_{\min}(\Sigma) = 0$ and $\|L\beta^*\|_\infty$ is bounded far away from 0, we encounter identifiability challenges which leads to an inconsistent estimator of β^* , just like the classical LASSO.

Remark 3.7. A natural question to consider is how the mean-squared error bound would change if the graph Laplacian penalty $\lambda_S \|\Gamma\beta\|_2^2$ were replaced by $\lambda_S \|\beta\|_2^2$ as is used in the Elastic Net ([Zou and Hastie, 2005](#)). Going through the analysis, $\lambda_{\min}(\Sigma + \lambda_S L)$ would be replaced by $\lambda_{\min}(\Sigma + \lambda_S I_{p \times p})$ and hence pre-conditioning is still achieved. However the important difference and why we prefer the graph Laplacian penalty is because using our analysis the condition $\lambda_1 \geq 8\lambda_S \|L\beta^*\|_\infty$ would be replaced by $\lambda_1 \geq 8\lambda_S \|\beta^*\|_\infty$. Hence if we were in the strictly sparse case and $\lambda_{TV} = 0$ we would recover the mean-squared error bound:

$$\|\hat{\beta} - \beta^*\|_2^2 \leq \frac{(\frac{\log p}{n} + \lambda_S^2 \|\beta^*\|_\infty^2) \|\beta^*\|_0}{\lambda_{\min}^2(\Sigma + \lambda_S I_{p \times p})}.$$

Note that this exactly matches the mean-squared error bound in (11) in [Hebiri and van de Geer \(2011\)](#) by replacing $\|\beta^*\|_2^2$ with the bound $\|\beta^*\|_0 \|\beta^*\|_\infty^2$. (The estimator of [Hebiri and van de Geer \(2011\)](#) is a generalization of the Elastic Net of [Zou and Hastie \(2005\)](#).) In general we can not expect $\|\beta^*\|_\infty$ to be close to zero which means we may have a consistent estimator, but in the case where β^* is well-aligned with L , we would expect $\|L\beta^*\|_\infty$ to be close to zero which would achieve sharper bounds.

Now we turn our attention to quantifying k_T and ρ to provide a more interpretable bound. We first have the following lemma to bound k_T :

Lemma 2. *Suppose $T = T_1 \cup T_2$ with $T_1 \subset \{p+1, p+2, \dots, p+m\}$ and $T_2 \subset \{1, 2, \dots, p\}$. Then we have*

$$k_T^{-1} \leq \frac{\lambda_{TV} \sqrt{2\|\hat{\Sigma}\|_{1,1}|T_1| + \sqrt{|T_2|}}}{\sqrt{|T_1| + |T_2|}}.$$

The proof for this lemma can be found in the Appendix.

Remark 3.8. The compatibility factor k_T depends on the choice of support T . Usually T will be chosen as $T = \text{Supp}(\tilde{\Gamma}\beta)$ for some β ; then $T_1 = \text{Supp}(\Gamma\beta)$ and $T_2 = \text{Supp}(\beta)$ and Lemma 2 can be reduced to

$$k_T^{-1} \leq \frac{\lambda_{\text{TV}} \sqrt{2\|\hat{\Sigma}\|_{1,1}\|\Gamma\beta\|_0 + \sqrt{\|\beta\|_0}}}{\sqrt{\|\Gamma\beta\|_0 + \|\beta\|_0}}.$$

To provide an upper bound for ρ we first define the following graph-based quantities. If G has K connected components where $1 \leq K \leq p$, L is block-diagonal with K blocks. Let L_k denote the k^{th} block of L , $B_k \subset \{1, 2, \dots, p\}$ denote the nodes corresponding to the k^{th} block, and μ_k denote the smallest non-zero eigenvalue of L_k .

Lemma 3. *Let G denote the graph associated with $\hat{\Sigma}$. Then*

$$\rho^2 \leq \max_{1 \leq k \leq K} \left\{ \frac{1}{|B_k|} + \frac{2}{1 + \mu_k \lambda_{\text{TV}}^2} \right\},$$

where K is the number of connected components in G ; $|B_k|$ is the corresponding number of nodes in B_k ; and μ_k is the smallest nonzero eigenvalue of the weighted Laplacian matrix for the k^{th} connected component.

The proof of Lemma 3 is provided in the Appendix.

Remark 3.9. Note that the definition of ρ for the edge-incidence matrix Γ was considered in Hütter and Rigollet (2016) while we define ρ for the modified matrix $\tilde{\Gamma}$, which involves both λ_{TV} and the identity matrix $I_{p \times p}$. Prior results in Hütter and Rigollet (2016) show that $\|\Gamma^\dagger\|_{1,2}^2 \leq \frac{1}{\mu_k}$, while Lemma 3 provides an upper bound for $\|\tilde{\Gamma}^\dagger\|_{1,2}^2$. In many cases, $\|\tilde{\Gamma}^\dagger\|_{1,2}^2 \ll \|\Gamma^\dagger\|_{1,2}^2$.

By combining results from Lemmas 2 and 3 we have the following theorem:

Theorem 2. *Under Assumptions 3.1 to 3.3 and we choose*

$$\lambda_1 \geq 48 \sqrt{\frac{\sigma^2 c_u \log p}{n}} \max_{1 \leq k \leq K} \left(\frac{1}{|B_k|} + \frac{2}{1 + \mu_k \lambda_{\text{TV}}^2} \right) + 8\lambda_S \|L\beta^*\|_\infty.$$

Then there exist absolute positive constants C_1 and C such that

$$\|\hat{\beta} - \beta^*\|_2^2 \leq C \frac{\lambda_1^2 \|\beta^*\|_0 + \min(\lambda_1^2 \lambda_{\text{TV}}^2 \|\hat{\Sigma}\|_{1,1} \|\Gamma\beta^*\|_0, \lambda_1 \lambda_{\text{TV}} \|\Gamma\beta^*\|_1)}{\min(\lambda_{\min}^2(\Sigma + \lambda_S L), \lambda_{\min}(\Sigma + \lambda_S L))},$$

with probability at least $1 - \frac{C_1}{p}$ provided $\frac{\lambda_1^2 \|\beta^*\|_0 + \lambda_1^2 \lambda_{\text{TV}}^2 \|\hat{\Sigma}\|_{1,1} \|\Gamma\beta^*\|_0}{\lambda_{\min}^2(\Sigma + \lambda_S L)} \rightarrow 0$ and $\lambda_1 \lambda_{\text{TV}} \|\Gamma\beta^*\|_1 \leq 1$.

The proof of Theorem 2 is provided in Section 6. The upper bound involves a minimum where one term depends on $\|\Gamma\beta^*\|_0$ and the other depends on $\|\Gamma\beta^*\|_1$ by using different choices of T . This minimum of two terms also appears in Hütter and Rigollet (2016). Theorem 2 captures the role of λ_{TV} and its impact on the mean-squared error (MSE) bounds. As λ_{TV} increases, $\|\beta^*\|_0$ contributes less to the MSE, while $\|\Gamma\beta^*\|_0$ or $\|\Gamma\beta^*\|_1$ contributes more. To see this, note that the lower bound condition on λ_1 decreases with λ_{TV} and the first term in the MSE scales as $\lambda_1^2 \|\beta^*\|_0$. On the other hand the second term of the MSE scales as $\lambda_1^2 \lambda_{\text{TV}}^2 \|\hat{\Sigma}\|_{1,1} \|\Gamma\beta^*\|_0$ or $\lambda_1 \lambda_{\text{TV}} \|\Gamma\beta^*\|_1$ and the lower bound on $\lambda_1 \lambda_{\text{TV}}$ increases as λ_{TV} increases.

3.1. Discussion of main results

If we are in the setting where $\lambda_{\min}(\Sigma) > C > 0$, which corresponds to the classical LASSO setting, then we set $\lambda_S = \lambda_{TV} = 0$. From Theorem 2 we can see that

$$\|\hat{\beta} - \beta^*\|_2^2 \preceq \frac{\sigma^2 c_u \log p}{n} \|\beta^*\|_0, \quad (10)$$

which is consistent with classical LASSO results. On the other hand if $\lambda_{\min}(\Sigma) \approx 0$ (columns are highly correlated) and $\|L\beta^*\|_\infty \approx 0$ (β^* is well-aligned with L), we can set $0 < \lambda_S \leq 1$ and $\lambda_{TV} = C \max_{1 \leq k \leq K} \sqrt{\frac{|B_k|}{\mu_k}}$; then we obtain the bound

$$\|\hat{\beta} - \beta^*\|_2^2 \preceq \lambda_1^2 \|\beta^*\|_0 + \min(\lambda_1^2 \lambda_{TV}^2 \|\hat{\Sigma}\|_{1,1} \|\Gamma\beta^*\|_0, \lambda_1 \lambda_{TV} \|\Gamma\beta^*\|_1)$$

where $\lambda_1^2 = O(\max_{1 \leq k \leq K} \frac{\sigma^2 c_u \log p}{n|B_k|})$ and $\lambda_1^2 \lambda_{TV}^2 = O(\max_{1 \leq k \leq K} \frac{|B_k|}{\mu_k} \max_{1 \leq k \leq K} \frac{\sigma^2 c_u \log p}{n|B_k|})$. The upper bound may be well below the classical LASSO bound in (10) when $\min_k |B_k| \gg 1$ if $\Gamma\beta^* \approx \mathbf{0}$.

As mentioned earlier, if $\lambda_{\min}(\Sigma) \approx 0$ (columns are highly correlated) but $\|L\beta^*\|_\infty > C > 0$ (bad alignment), our method cannot guarantee a consistent estimator for β^* ; Cluster Representative LASSO and Ordered Weighted LASSO will also fail in this case. Identifiability assumptions arise, since if two columns of X are nearly identical but the corresponding elements of β^* are substantially different, no method will be able to accurately estimate parameter values in the absence of additional structure.

We now discuss the roles of the various parameters associated with the MSE bound.

Role of λ_S : The smoothing penalty plays the role of a pre-conditioner where the trade-off is the addition of another term $\lambda_S \|L\beta^*\|_\infty$. This can also be seen in the optimization problem (5) where X is transformed to \tilde{X} , so even if the restricted eigenvalue condition is not satisfied for X , it is satisfied for \tilde{X} . What distinguishes our results from previous work using pre-conditioners for the LASSO (Jia et al., 2015; Wauthier, Jojic and Jordan, 2013) is that prior work does not address the case where $\lambda_{\min}(\Sigma) = 0$, which is where the total variation penalty is important. See also Remark 3.7.

Role of λ_{TV} : As mentioned earlier, the total variation penalty promotes estimates well-aligned with the graph. As λ_{TV} increases, the sparsity parameter λ_1 decreases while $\lambda_1 \lambda_{TV}$ increases. By increasing λ_{TV} we can also adapt to settings where β^* is not sparse provided that $\Gamma\beta^*$ is sparse (see the example of the block covariance graph below).

Graph-based quantities: Two important parameters of the covariance graph are μ_k (the smallest non-zero eigenvalue of a block) and $|B_k|$ (the block size). Clearly the larger μ_k and $|B_k|$, the lower the bound on λ_1 which potentially suggests lower mean-squared error. On the other hand, as we illustrate with specific examples later, larger μ_k typically indicates higher correlation between more covariates and larger $|B_k|$ corresponds to nodes being correlated, which means $\lambda_{\min}(\Sigma)$ is smaller.

3.2. Specific covariance graph structures

In this section we explore two different specific graph structures and discuss suitable choices of λ_S , λ_1 and λ_{TV} . For each graph structure we assume

$$\Sigma_{jj} = a > 0 \text{ for } 1 \leq j \leq p \quad \text{and} \quad \Sigma_{jk} = ar \ \forall (j, k) \in E \text{ for some } 0 < r \leq 1;$$

we refer to r as the correlation coefficient. Note that here a is a normalization parameter that we set to ensure such that Assumptions 3.1 and 3.2 are satisfied. We will talk about the specific choices of a for each graph structure below. For interpretability and simplicity of exposition, we further assume that $\hat{\Sigma} = \Sigma$ – that is, that we have side information about the correlation graph.

3.2.1. Block covariance graph

We first consider a block complete graph G that has K connected components and each connected component is a complete graph with $\frac{p}{K}$ nodes. The corresponding covariance matrix Σ (potentially after a suitable permutation of rows and columns) is block diagonal with K blocks of size $\frac{p}{K} \times \frac{p}{K}$. Each of these blocks can be written as

$$ar \mathbb{1}_{p/K} \mathbb{1}_{p/K}^\top + a(1-r)I_{p/K},$$

where $\mathbb{1}_{p/K}$ is the vector of p/K ones. We set $a = \frac{K}{p}$ to ensure that Assumptions 3.1 and 3.2 are satisfied. In the extreme case where $K = p$, we are in the independent case and the estimator reduces to the standard LASSO estimator; whereas for $K = 1$, we are in the fully-connected graph case. Figure 1 illustrates an example with $p = 16$ and $K = 4$ along with the corresponding Σ .

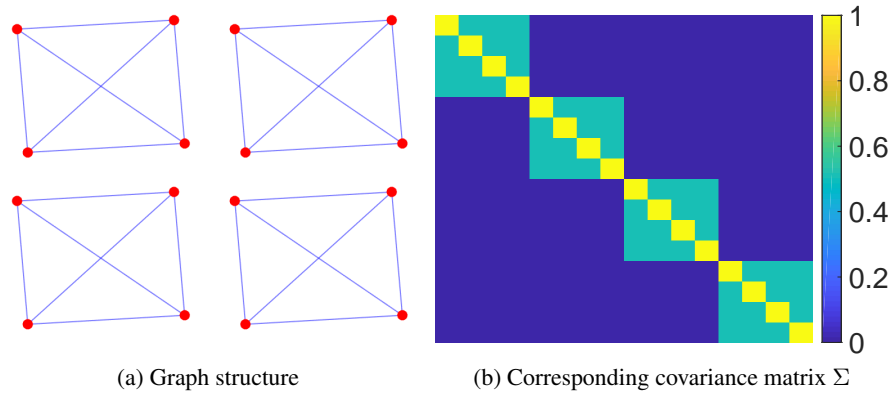


FIG 1. Block complete graph with $p = 16$ and $K = 4$.

Thus we have the following lemma to provide specific bounds on $\max_{1 \leq k \leq K} \frac{1}{|B_k|}$, μ_k , ρ , $\lambda_{\min}(\Sigma + \lambda_S L)$:

Lemma 4. For a block complete graph with details described above, suppose that $\hat{\Sigma} = \Sigma$ then we have

$$\begin{aligned} \max_{1 \leq k \leq K} \frac{1}{|B_k|} &= \frac{K}{p}, \\ \mu_k &= r, \text{ for all } k \\ \rho &\leq \sqrt{\frac{K}{p} + \frac{2}{1 + r\lambda_{TV}^2}}, \\ \lambda_{\min}(\Sigma + \lambda_S L) &\geq (1 - \lambda_S)(1 - r)\frac{K}{p} + \lambda_S r. \end{aligned}$$

The proof of Lemma 4 is deferred to the Appendix. Note that if $r = 1$, $\lambda_{\min}(\Sigma) = 0$ but $\lambda_{\min}(\Sigma + \lambda_S L) \geq \lambda_S$. Using Lemma 4, we have the following mean-squared error bound for the block complete graph:

Corollary 1. Suppose that Assumptions 3.1 and 3.2 are satisfied and $\hat{\Sigma} = \Sigma$. If

$$\lambda_1 \geq 48 \sqrt{\frac{\sigma^2 c_u \log p}{n} \left(\frac{K}{p} + \frac{2}{1 + r\lambda_{TV}^2} \right)} + 8\lambda_S \|L\beta^*\|_\infty$$

and $\lambda_1 \lambda_{TV} \|\Gamma \beta^*\|_1 \leq 1$. Then with probability at least $1 - \frac{C_1}{p}$

$$\|\hat{\beta} - \beta^*\|_2^2 \leq \frac{C(\lambda_1^2 \|\beta^*\|_0 + \min\{\lambda_1^2 \lambda_{TV}^2 \|\Gamma \beta^*\|_0, \lambda_1 \lambda_{TV} \|\Gamma \beta^*\|_1\})}{\min\{[(1 - \lambda_S)(1 - r)\frac{K}{p} + \lambda_S r], [(1 - \lambda_S)(1 - r)\frac{K}{p} + \lambda_S r]^2\}}$$

given the estimator is consistent, where C_1, C are absolute positive constants.

Note that for $r \approx 1$ and $\Gamma \beta^* \approx \mathbf{0}$ (near-perfect alignment which corresponds to the parameters in each block having the same values), if we choose $\lambda_S > 0$, $\lambda_{TV}^2 \succeq \frac{p}{K}$, and $\lambda_1^2 = O(\frac{K \log p}{pn})$, then

$$\|\hat{\beta} - \beta^*\|_2^2 \preceq \frac{K \log p}{n};$$

that is, the MSE is not determined by the number of nonzeros in β^* , but rather by K , the number of clusters of nodes. A similar scaling was derived in [Figueiredo and Nowak \(2016\)](#) also under the assumption that $\Gamma \beta^* \approx \mathbf{0}$.

3.2.2. Chain covariance graph

The chain graph is illustrated in Figure 2. The corresponding covariance matrix (perhaps after a suitable permutation of the rows and columns) satisfies $\Sigma_{jk} = ar$ for all $(j, k) \in E$ where $E = \{(1, 2), (2, 3), \dots, (p - 1, p)\}$. Requiring $r \in (0, \frac{1}{2})$ ensures Σ is positive semi-definite. Note that for the chain graph when $a = 1$ Assumption 3.1 is satisfied for any $r \in (0, \frac{1}{2})$, thus in the following discussion we set $a = 1$. Assumption 3.2 is also satisfied if we set $a = 1$. Note that the chain graph is fully connected so $K = 1$ and $B_1 = \{1, 2, \dots, p\}$.

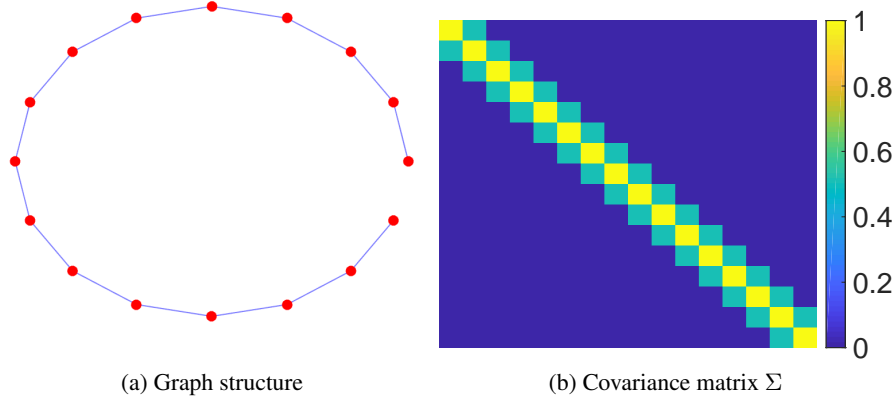


FIG 2. Chain graph with $p = 16$

Thus we have the following lemma to provide specific bounds on $\frac{1}{|B_1|}, \mu_1, \rho, \lambda_{\min}(\Sigma + \lambda_S L)$ for the chain covariance graph:

Lemma 5. For a chain graph with details described above, suppose that $\hat{\Sigma} = \Sigma$. Then

$$\begin{aligned} \frac{1}{|B_1|} &= \frac{1}{p}, \\ \mu_1 &= (2 - 2 \cos(\frac{\pi}{p}))r, \\ \rho &\leq \sqrt{\frac{1}{p} + \frac{2}{1 + (2 - 2 \cos(\frac{\pi}{p}))r\lambda_{TV}^2}}, \\ \lambda_{\min}(\Sigma + \lambda_S \Gamma^\top \Gamma) &\geq (1 - \lambda_S)(1 - 2r) + \lambda_S. \end{aligned}$$

The proof of Lemma 5 is deferred to the Appendix. Hence we have the following corollary for the chain graph:

Corollary 2. Suppose Assumptions 3.1 and 3.2 are satisfied, and $\hat{\Sigma} = \Sigma$. If we choose

$$\lambda_1 > 48 \sqrt{\frac{\sigma^2 c_u \log p}{n} \left(\frac{1}{p} + \frac{2}{1 + (2 - 2 \cos(\frac{\pi}{p}))r\lambda_{TV}^2} \right)} + 8\lambda_S \|L\beta^*\|_\infty$$

and $\lambda_1 \lambda_{TV} \|\Gamma\beta^*\|_1 \leq 1$, then with probability at least $1 - \frac{C_1}{p}$ we have

$$\|\hat{\beta} - \beta^*\|_2^2 \leq \frac{C(\lambda_1^2 \|\beta^*\|_0 + \min\{\lambda_1^2 \lambda_{TV}^2 \|\Gamma\beta^*\|_0, \lambda_1 \lambda_{TV} \|\Gamma\beta^*\|_1\})}{\min\{[(1 - \lambda_S)(1 - 2r) + \lambda_S], [(1 - \lambda_S)(1 - 2r) + \lambda_S]^2\}}$$

given the estimator is consistent, where C_1, C are absolute positive constants.

There are three interesting regimes of λ_{TV} that are applicable for different sparsity and alignment assumptions on β^* . In particular, (i) if $\lambda_{TV} = 0$, ρ scales as a constant, and the mean-squared error scales as $\lambda_1^2 \|\beta^*\|_0$. Hence if β^* is sparse, we achieve consistent estimation with $\lambda_{TV} = 0$ if either the correlation is weak ($\lambda_S \approx 0$) or β^* and Σ are well-aligned ($\|L\beta^*\|_\infty \approx 0$). On the other hand, (ii) if $\lambda_{TV}^2 \succeq \frac{p}{(2 - 2 \cos(\pi/p))r}$, ρ^2 scales as $\frac{1}{p}$, $\lambda_1^2 \asymp \frac{\log p}{np} + \lambda_S^2 \|L\beta^*\|_\infty^2$, and the mean-squared error scales as $\frac{\|\beta^*\|_0 \log p}{np} + \lambda_S^2 \|L\beta^*\|_\infty^2 \|\beta^*\|_0 + \min(\lambda_1^2 \lambda_{TV}^2 \|\Gamma\beta^*\|_0, \lambda_1 \lambda_{TV} \|\Gamma\beta^*\|_1)$. Hence if $\Gamma\beta^* = \mathbf{0}$ we have $\|\beta^*\|_0 = p$, we can then achieve a mean-squared error of $O(\frac{\log p}{n})$. Finally, (iii) if $\lambda_{TV}^2 \preceq \frac{p}{(2 - 2 \cos(\pi/p))r}$, ρ^2 scales as $\frac{2}{1 + (2 - 2 \cos(\pi/p))r\lambda_{TV}^2}$, $\lambda_1^2 \asymp \frac{\rho^2 \log p}{n} + \lambda_S^2 \|L\beta^*\|_\infty^2$, and the mean-squared error scales as $\frac{\rho^2 \|\beta^*\|_0 \log p}{n} + \lambda_S^2 \|L\beta^*\|_\infty^2 \|\beta^*\|_0 + \min(\lambda_1^2 \lambda_{TV}^2 \|\Gamma\beta^*\|_0, \lambda_1 \lambda_{TV} \|\Gamma\beta^*\|_1)$. As noted in Hütter and Rigollet (2016), the chain graph is a particularly challenging setting for achieving fast rates, even in the denoising setting.

4. Simulation study

In this section we compare our proposed graph-based regularization method with other methods on two different graph structures: the block complete graph and chain graph considered in the corollaries above. In our simulations, the graphs and corresponding covariance structures are constructed as follows:

Block Complete Graph: Σ is block diagonal with K blocks, each of size $\frac{p}{K} \times \frac{p}{K}$. Following discussion in Section 3.2.1, all the diagonal elements are set to $\frac{K}{p}$ and all the off-diagonal elements in each block are set to $\frac{Kr}{p}$ with $r \in (0, 1)$. Here, r is the correlation coefficient and will be set to different values in the experiments. Specifically, let

$$B = \frac{K}{p} \left(r \mathbb{1}_{p/K} \mathbb{1}_{p/K}^\top + (1 - r) I_{p/K} \right) \quad \text{and} \quad \Sigma = I_K \otimes B,$$

where \otimes denotes the Kronecker product. To set the true coefficient vector β^* , we first randomly choose ℓ of the K blocks to be “active blocks” and all the rest blocks are inactive. Then we set the elements in β^* that correspond to the ℓ active blocks to be $\beta_j^* \sim \mathcal{N}(1, 0.01^2)$ when i belongs to these ℓ active blocks and all other elements in β^* to be 0 (inactive). That is, let $S \in \{0, 1\}^p$ indicate the indices in active blocks (and hence the support of β^*); then

$$\beta^* \sim \mathcal{N}(S, 0.01^2 \text{diag}(S)).$$

Chain Graph: Following the discussion in Section 3.2.2, we set elements in the main diagonal of Σ to be one, the first off-diagonal elements to be r with $r \in (0, \frac{1}{2})$, and all the other elements to be zero; *i.e.*,

$$\Sigma_{j,k} = \begin{cases} 1, & \text{if } j = k, \\ r, & \text{if } |j - k| = 1, \\ 0, & \text{else.} \end{cases}$$

The corresponding true coefficient vector β^* is set to have $\beta_j^* \sim \mathcal{N}(1, 0.01^2)$ for $1 \leq j \leq s$ and the remaining elements to be zero. That is, let $S \in \{0, 1\}^p$ have its first $s < p$ elements be one and the remaining be zero; then

$$\beta^* \sim \mathcal{N}(S, 0.01^2 \text{diag}(S)).$$

The data is generated according to $y = X\beta^* + \epsilon$ with $X \in \mathbb{R}^{n \times p}$ and $y \in \mathbb{R}^n$. Each row of X is independently generated from $\mathcal{N}(\mathbf{0}, \Sigma_{p \times p})$ and ϵ is generated from $\mathcal{N}(\mathbf{0}, \sigma^2 I_{n \times n})$ with $\sigma = 0.01$. Additionally, we generate $X_{\text{ind}} \in \mathbb{R}^{1000 \times p}$ with each row of X_{ind} independently generated from $\mathcal{N}(\mathbf{0}, \Sigma_{p \times p})$. This X_{ind} provides side information that can be used to improve estimates of Σ . This X_{ind} can be used for covariance estimation (GTV) or clustering (CRL) before parameter estimation.

We show how our proposed graph-based regularization scheme compares to existing state-of-the-art methods in terms of mean-squared error $\text{MSE} = \|\hat{\beta} - \beta^*\|_2^2$. For all methods, tuning parameters are chosen based on five-fold cross-validation. In particular we consider the following estimation procedures:

GTV-Esti (Our method): Graph-based total variation (GTV) method using original design matrix $X \in \mathbb{R}^{n \times p}$ for both covariance matrix estimation and parameter estimation. To implement GTV-Esti, we first use X to compute the estimated covariance matrix, $\hat{\Sigma}$, using hard thresholding of the sample covariance matrix with a threshold is chosen by cross validation (see [Bickel and Levina \(2008b\)](#) for more details). We construct the edge incidence matrix Γ based on $\hat{\Sigma}$ and then estimate $\hat{\beta}$ using (5).

GTV-Indep (Our method): This approach is equivalent to GTV-Esti (above), except that the side information X_{ind} is used to compute the estimated covariance matrix $\hat{\Sigma}$.

CRL-Esti: Cluster Representative LASSO (CRL) method of [Bühlmann et al. \(2013\)](#) using X for both covariate clustering and parameter estimation. To implement CRL-Esti, we first use X for covariate clustering using canonical correlations in X (see [Bühlmann et al. \(2013, Algorithm 1\)](#) for more details), then the Cluster Representative LASSO is implemented based on the clusters.

CRL-Indep: This approach is equivalent to CRL-Eesti (above), except that the side information X_{ind} is used to improve clustering of the covariates. That is, we run CRL as before, but based on the canonical correlations computed from X_{ind} .

LASSO: Standard LASSO ([Tibshirani, 1996](#)).

OWL: Ordered Weighted LASSO ([Figueiredo and Nowak, 2016](#)). We set the weights for OWL corresponding to the OSCAR regularizer ([Bondell and Reich, 2008](#)), *i.e.*, $w_i = \lambda_1 + \lambda_2(p - i)$ with $1 \leq i \leq p$ and $\lambda_1, \lambda_2 \geq 0$.

We want to investigate how the mean-squared error (MSE) changes with number of observations n , number of covariates p , support size of the true coefficient vector $s = \|\beta^*\|_0$, and the correlation coefficient r between covariates.

For each graph structure we consider the following configurations in our simulation:

MSE vs. n : We choose $n \in \{60, 70, 80, 90, 100, 110, 120\}$ and set $p = 280$. For the block graph we set $K = 20$, $r = 0.7$, and the number of active blocks is 6 ($s = 6p/K = 84$); for the chain graph we set $s = 80$ and $r = 0.4$. See Figure 3.

MSE vs. p : We choose $p \in \{80, 120, 160, 200, 240, 280, 320\}$ and set $n = 100$. For the block graph we set $K = 20$, $r = 0.7$, and the number of active blocks is 6; for the chain graph we set $s = 80$ and $r = 0.4$. See Figure 4.

MSE vs. s : We set $p = 280$ and $n = 100$. For the block graph we set $K = 20$, $r = 0.7$ and the number of active blocks is in the set $\{2, 3, 4, 5, 6, 7, 8\}$ (so $s \in \{28, 42, 56, 70, 84, 98, 112\}$); for the chain graph we set $r = 0.4$ and $s \in \{40, 50, 60, 70, 80, 90, 100\}$. See Figure 5.

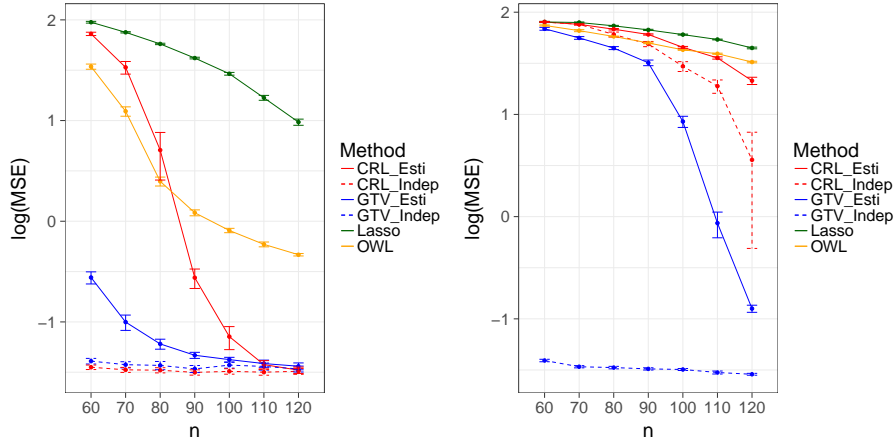
MSE vs. r : We set $p = 280$ and $n = 100$. For the block graph we set $K = 20$, the number of active blocks is 6 ($s = 84$), and $r \in \{0.3, 0.4, 0.5, 0.6, 0.7, 0.8, 0.9\}$; for the chain graph we set $s = 80$ and $r \in \{0.15, 0.2, 0.25, 0.3, 0.35, 0.4, 0.45\}$. See Figures 6.

The results are summarized in Figures 3-6. We show the median MSE of 100 trials and we add error bars with the standard deviation (of the median) estimated using the bootstrap method with 500 resamplings on the 100 MSEs. It can be seen that for almost all cases GTV-Esti has lower MSE than CRL-Esti, OWL and LASSO; if we have additional side information we can achieve better results by using GTV-Indep or CRL-Indep. We can also see that the MSE decreases as n increases and MSE increases as p or s increases, which is consistent with our theoretical results. To investigate the relationship between MSE and correlation coefficient r , for the block graph we can see that GTV-Esti, CRL-Esti and OWL have lower MSE when r increases; this phenomenon is reasonable since when r increases it will be easier for these methods to capture true cluster information from X and then the results will be better; and in the chain graph we can see GTV-Esti has lower MSE when r increases but MSE for CRL-Esti, OWL and LASSO have no significant changes. In particular, note that the CRL requires one to cluster features *independently of label information in y* , and for the chain graph there are no clear clusters. In contrast, GTV is essentially clustering features based on both the covariance structure in $\hat{\Sigma}$ and the label information in y , so that a group of active elements in β^* on a subset of the chain can be correctly identified as a cluster.

We also provide a comparison about the behavior of estimators by six different methods for each graph structure. The results are shown in Figure 7 and 8. For both cases we can see that GTV methods (both with and without side information) outperform the other methods in terms of recovering the true structure of β^* . Figure 7 shows that in the block graph setting, the LASSO and CRL-Esti struggle to recover the signal structure and OWL produces slightly noisier estimates than GTV; the other three methods successfully recover the true signal structure. From Figure 8, we can see in the chain graph setting that only GTV-Indep and GTV-Esti achieve satisfactory results for recovering true signal β^* .

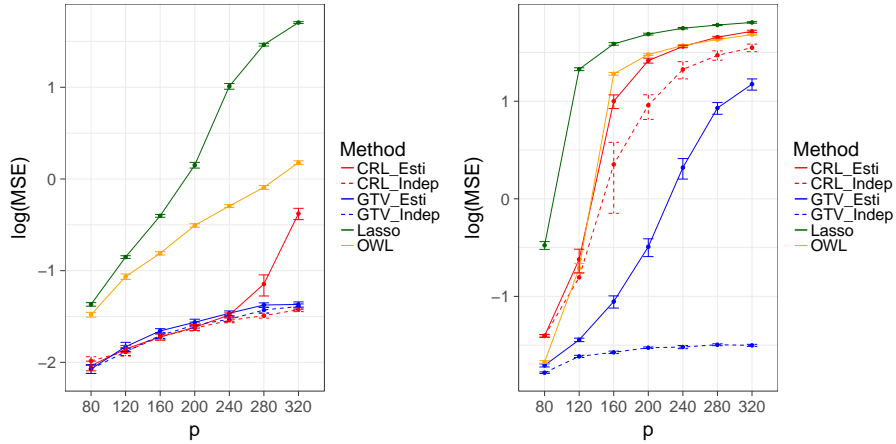
5. Application to real fMRI data

In this section we describe the application of the proposed GTV methodology to neural decoding with fMRI data. The fMRI data we use is provided by the Postle Lab in UW-Madison (Lewis-Peacock and Postle, 2008). The data contains fMRI measurements for ten different participants. Each participant takes part in an fMRI experiment with ninety trials, where for each trial the participant views a picture of either a human face or something with no human face present. fMRI blood-oxygen-level dependent (BOLD) signals corresponding to these ninety trials are recorded when the participant is looking at these pictures,



(a) Block Graph ($p = 280, s = 84, r = 0.7$) (b) Chain Graph ($p = 280, s = 80, r = 0.4$)

FIG 3. MSE (log scale) vs. n for (a) block graph and (b) chain graph. Median of 100 trials are shown, and error bars denote the standard deviation of the median estimated by using the bootstrap with 500 resamplings on the 100 mean-squared errors. The six different methods are: (1) Graph-based total variation method with covariance matrix estimated from X (GTV-Esti); (2) Graph-based total variation method with covariance matrix estimated from X_{ind} (GTV-Indep); (3) Cluster Representative LASSO (Bühlmann et al. (2013)) with clustering based on X (CRL-Esti); (4) Cluster Representative LASSO with clustering based on X_{ind} (CRL-Indep); (5) LASSO (Tibshirani, 1996); (6) Ordered Weighted LASSO (OWL, Figueiredo and Nowak (2016)). MSE decreases when n increases for GTV-Esti, which is consistent with our theory, and yields lower MSEs than other methods for a broad range of n .



(a) Block Graph ($n = 100$, Active blocks = 6, (b) Chain Graph ($n = 100, s = 80, r = 0.4$)
 $r = 0.7$)

FIG 4. MSE (log scale) vs. p for (a) block graph and (b) chain graph. Median of 100 trials are shown, and error bars denote the standard deviation of the median estimated by using the bootstrap with 500 resamplings on the 100 mean-squared errors. The six different methods are: (1) Graph-based total variation method with covariance matrix estimated from X (GTV-Esti); (2) Graph-based total variation method with covariance matrix estimated from X_{ind} (GTV-Indep); (3) Cluster Representative LASSO (Bühlmann et al. (2013)) with clustering based on X (CRL-Esti); (4) Cluster Representative LASSO with clustering based on X_{ind} (CRL-Indep); (5) LASSO (Tibshirani, 1996); (6) Ordered Weighted LASSO (OWL, Figueiredo and Nowak (2016)). MSE increases when p increases for GTV-Esti, which is consistent with our theory, and yields lower MSEs than other methods for a broad range of p , particularly in the chain graph.

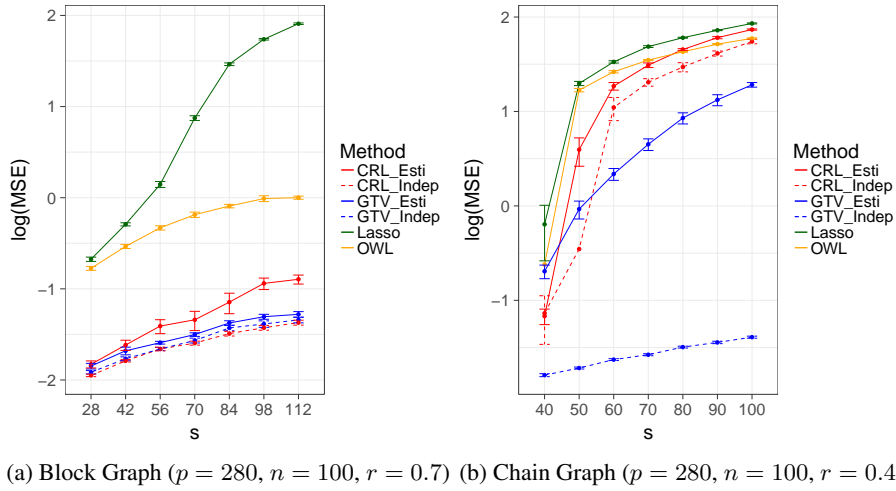


FIG 5. MSE (log scale) vs. s for (a) block graph and (b) chain graph. Median of 100 trials are shown, and error bars denote the standard deviation of the median estimated by using the bootstrap with 500 resamplings on the 100 mean-squared errors. The six different methods are: (1) Graph-based total variation method with covariance matrix estimated from X (GTV-Esti); (2) Graph-based total variation method with covariance matrix estimated from X_{ind} (GTV-Indep); (3) Cluster Representative LASSO (Bühlmann et al. (2013)) with clustering based on X (CRL-Esti); (4) Cluster Representative LASSO with clustering based on X_{ind} (CRL-Indep); (5) LASSO (Tibshirani, 1996); (6) Ordered Weighted LASSO (OWL, Figueiredo and Nowak (2016)). We can see that MSE increases when s increases for GTV-Esti, which is consistent with our theory, and yields lower MSEs than other methods for a broad range of s , particularly in the chain graph.

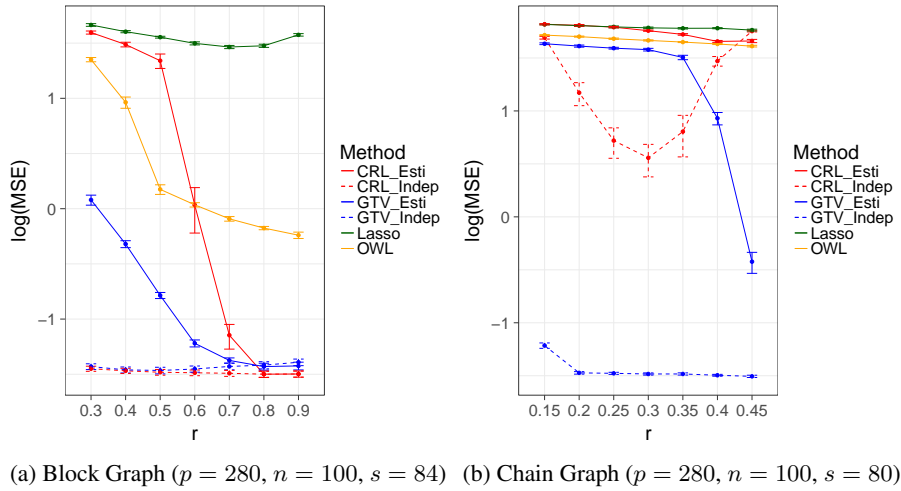


FIG 6. MSE (log scale) vs. r for (a) block graph and (b) chain graph. Median of 100 trials are shown, and error bars denote the standard deviation of the median estimated by using the bootstrap with 500 resamplings on the 100 mean-squared errors. The six different methods are: (1) Graph-based total variation method with covariance matrix estimated from X (GTV-Esti); (2) Graph-based total variation method with covariance matrix estimated from X_{ind} (GTV-Indep); (3) Cluster Representative LASSO (Bühlmann et al. (2013)) with clustering based on X (CRL-Esti); (4) Cluster Representative LASSO with clustering based on X_{ind} (CRL-Indep); (5) LASSO (Tibshirani, 1996); (6) Ordered Weighted LASSO (OWL, Figueiredo and Nowak (2016)). We can see that MSE decreases when r increases for GTV-Esti, which is consistent with our theory.

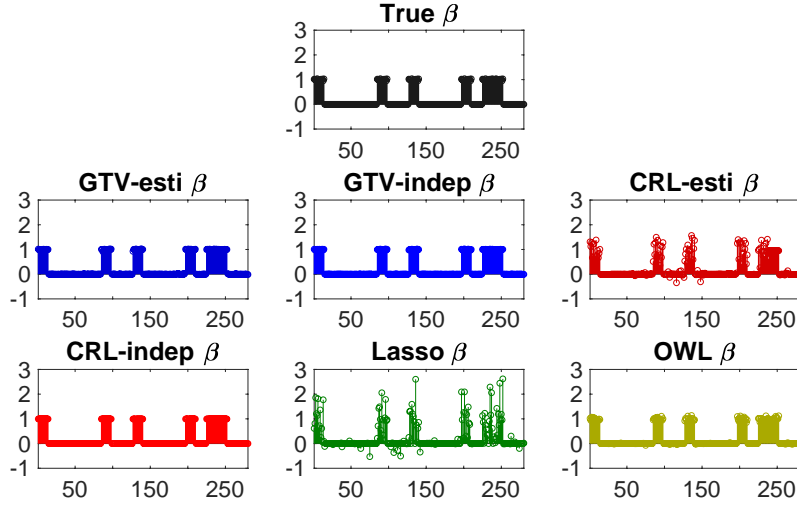


FIG 7. Comparison of six different estimator's behavior for block graph setting (with simulation parameters $p = 280, n = 100, s = 84, r = 0.6$). The six different methods are: (1) Graph-based total variation method with covariance matrix estimated from X (GTV-Esti); (2) Graph-based total variation method with covariance matrix estimated from X_{ind} (GTV-Indep); (3) Cluster Representative LASSO (Bühlmann et al. (2013)) with clustering based on X (CRL-Esti); (4) Cluster Representative LASSO with clustering based on X_{ind} (CRL-Indep); (5) LASSO (Tibshirani, 1996); (6) Ordered Weighted LASSO (OWL, Figueiredo and Nowak (2016)). We can see that except for LASSO and CRL-Esti, other methods can approximately recover the true signal structure.

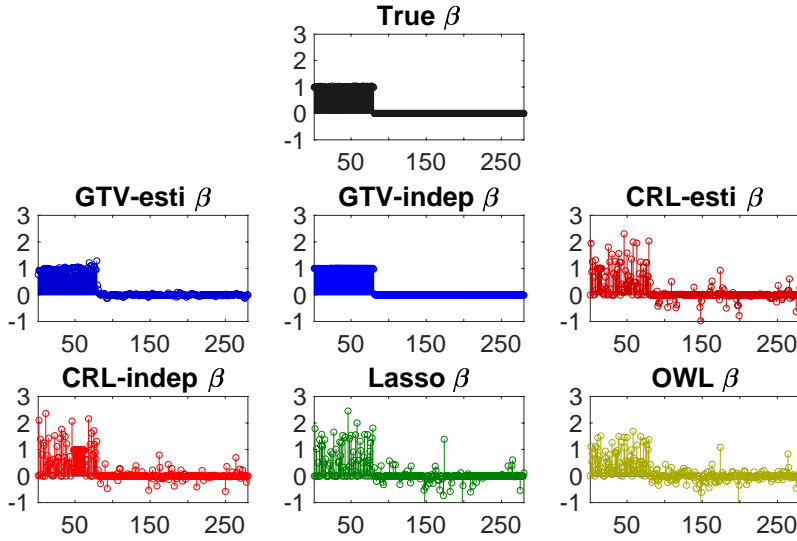


FIG 8. Comparison of six different estimator's behavior for chain graph setting (with simulation parameters $p = 280, n = 100, s = 80, r = 0.45$). The six different methods are: (1) Graph-based total variation method with covariance matrix estimated from X (GTV-Esti); (2) Graph-based total variation method with covariance matrix estimated from X_{ind} (GTV-Indep); (3) Cluster Representative LASSO (Bühlmann et al. (2013)) with clustering based on X (CRL-Esti); (4) Cluster Representative LASSO with clustering based on X_{ind} (CRL-Indep); (5) LASSO (Tibshirani, 1996); (6) Ordered Weighted LASSO (OWL, Figueiredo and Nowak (2016)). We can see that only GTV-Indep and GTV-Esti can approximately recover the true signal structure.

and for each voxel we compute how well the measured bold signal fits a signal template corresponding to the expected hemodynamic response to a visual stimulus. We model each individual separately. There is a parameter associated with each (trial,voxel) pair are stored in a matrix $X \in \mathbb{R}^{90 \times p}$, where p is the number of voxels in the brain recorded for the individual and the values of p for ten participants are: {7303, 5179, 4176, 5651, 5847, 8082, 4101, 6600, 9111, 7193}.

We normalize this fMRI data matrix X such that each column has unit Euclidean norm before analysis. For each participant we also have the response variable $y \in \mathbb{R}^{90}$ which records each picture as a “face” picture or not for each trial; $y = 1$ if this picture is “face” picture and $y = 0$ otherwise. Although the responses are binary, we use the least-squares loss based on the original objective function. For each participant, the Postle Lab also provides a time series version of the fMRI measurements $X_{\text{TS}} \in \mathbb{R}^{1170 \times p}$. This X_{TS} matrix contains the entire BOLD signal for the entirety of the fMRI experiment.

5.1. Implementation for GTV

To implement our GTV method on the fMRI dataset, we use X_{TS} to estimate the covariance matrix. We first normalize X_{TS} such that each column has unit Euclidean norm. Then we estimate the covariance matrix by using a diagonal plus low-rank matrix decomposition (Saunderson et al. (2012), with connections to the spiked covariance model Donoho, Gavish and Johnstone (2013); Baik and Silverstein (2006)) which seemed to fit this data; we denote this estimator $\hat{\Sigma}$. The resulting covariance estimate $\hat{\Sigma}$ is not necessarily sparse. If the estimated covariance matrix is dense, there are $O(p^2)$ terms in (2), affecting the speed of the computation of both the smoothing penalty and the total variation penalty. For faster computation, instead of using the entire estimated covariance matrix for the graph-based regularizers, we obtain a *skeleton graph* for G and define $\hat{\Sigma}$ with respect to this graph, which reduces the number of terms in (2) to $O(p)$. Our idea is to find a skeleton graph with maximum possible total absolute edge weight. Thus we obtain a skeleton tree graph G_T through the following three steps: (1) Define $\hat{\Sigma}^{\text{Pos}} \in \mathbb{R}^{p \times p}$ with $\hat{\Sigma}_{j,k}^{\text{Pos}} = |\hat{\Sigma}_{j,k}|$ for $1 \leq j, k \leq p$; (2) Find a maximum spanning tree G_{MST} based on this matrix $\hat{\Sigma}^{\text{Pos}}$ by implementing Prim’s algorithm (Prim, 1957) based on a greedy search; (3) For each edge (j, k) in the maximum spanning tree G_{MST} , replace the edge weight $\hat{\Sigma}_{j,k}^{\text{Pos}}$ by $\hat{\Sigma}_{j,k}$, and we call this new tree graph with updated edge weights to be G_T . Then the smoothing and total variation penalties in GTV method can be implemented based on this tree graph G_T to solve the computation issues.

5.2. Results

We compare our GTV method with Ordered Weighted LASSO (OWL, Figueiredo and Nowak (2016)), Cluster Representative LASSO (CRL, Bühlmann et al. (2013)) and the standard LASSO method (Tibshirani, 1996). According to Lewis-Peacock and Postle (2008), for each participant the order of showing ninety pictures is random, thus we use fMRI data corresponding to the first sixty trials as training set X_{train} and fMRI data corresponding to the remaining thirty trials as testing set X_{test} . For all four models, tuning parameters were set using five-fold cross validation. The classification accuracy results of these four methods on the testing set are summarized in Figure 9, which shows that GTV has highest classification accuracy among all methods for eight participants out of ten. CRL has similar results to the LASSO since in the clustering step CRL does not create many big clusters for covariates. OWL has better performance than CRL and LASSO in terms of classification accuracy and is closest in accuracy to GTV.

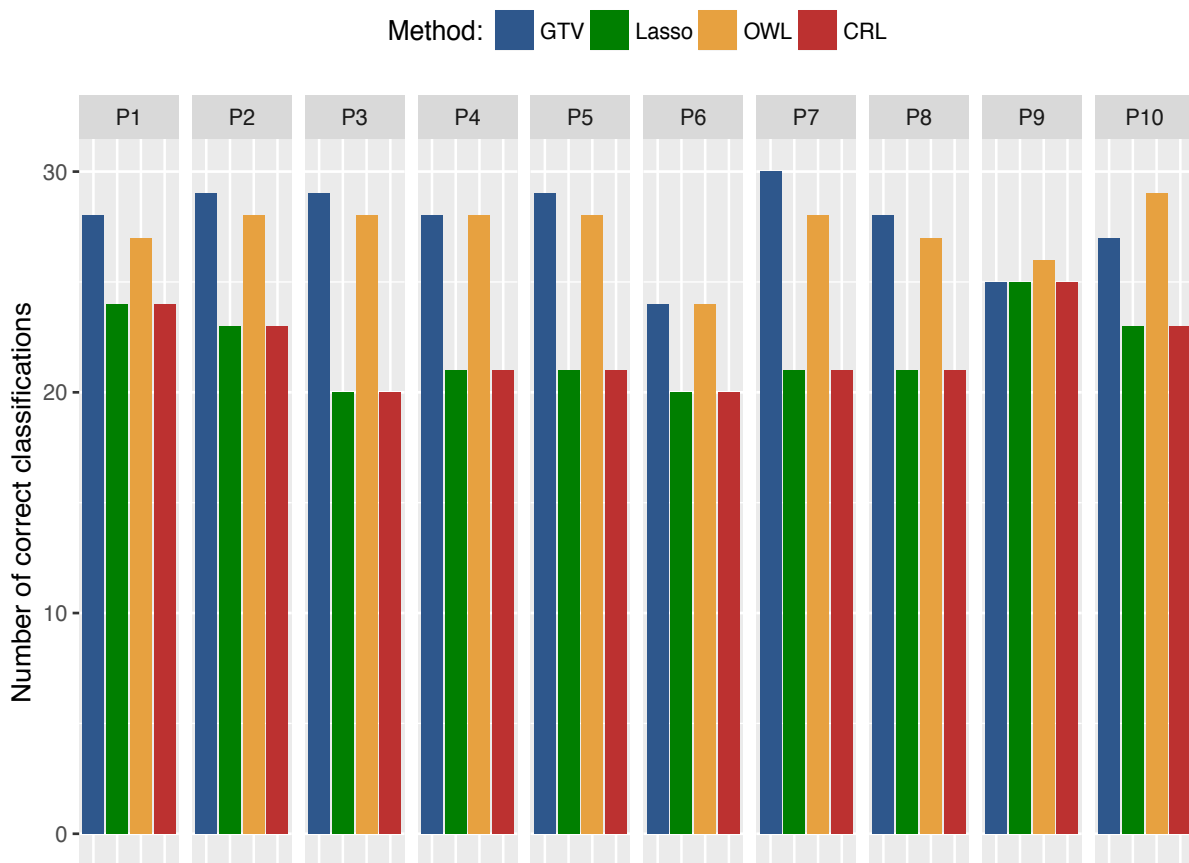


FIG 9. Classification accuracy for four different methods applied to an fMRI study in which participants were asked to view images of faces and non-faces, described in Section 5. The four different color bars correspond to four different methods: (1) Graph-based total variation (GTV, this paper); (2) LASSO (Tibshirani, 1996); (3) Ordered Weighted LASSO (OWL, Figueiredo and Nowak (2016)); (4) Cluster Representative LASSO (CRL, Bühlmann et al. (2013)). The horizontal axis represents ten different participants denoted from P1 to P10 and the vertical axis represents number of correct classifications for each method. GTV achieves highest classification accuracy among all four methods for eight participants out of ten. Random guessing would yield an average of fifteen correct classifications per participant.

6. Proofs

6.1. Proof of Theorem 1

The proof involves direct analysis of the lasso estimator and techniques from [Hütter and Rigollet \(2016\)](#) and [Raskutti and Yuan \(2015\)](#). Our analysis follows standard steps for analysis of regularized M-estimators (cf., [Bickel, Ritov and Tsybakov \(2009\)](#); [Negahban et al. \(2012\)](#); [van de Geer \(2000\)](#)) along with addressing two challenges specific to this setting: (1) since here the regularizer is $\|\tilde{\Gamma}\beta\|_1$ which is not $\|\beta\|_1$, we need to deal with error terms involving $\tilde{X}\tilde{\Gamma}^\dagger$ instead of \tilde{X} which we will address using techniques from [Hütter and Rigollet \(2016\)](#) to control and [Raskutti and Yuan \(2015\)](#); (2) using techniques in [Raskutti, Wainwright and Yu \(2010\)](#), we control the restricted eigenvalue condition for \tilde{X} rather than X .

Based on the optimization problem (5), by the definition of $\hat{\beta}$ and the basic inequality,

$$\frac{1}{n}\|\tilde{y} - \tilde{X}\hat{\beta}\|_2^2 + \lambda_1\|\tilde{\Gamma}\hat{\beta}\|_1 \leq \frac{1}{n}\|\tilde{y} - \tilde{X}\beta^*\|_2^2 + \lambda_1\|\tilde{\Gamma}\beta^*\|_1.$$

By simple re-arrangement,

$$\frac{1}{n}\|\tilde{X}(\hat{\beta} - \beta^*)\|_2^2 \leq \frac{2}{n}(\tilde{y} - \tilde{X}\beta^*)^\top \tilde{X}(\hat{\beta} - \beta^*) + \lambda_1(\|\tilde{\Gamma}\beta^*\|_1 - \|\tilde{\Gamma}\hat{\beta}\|_1).$$

For the remainder of the proof let $\Delta := \hat{\beta} - \beta^*$. Then

$$\frac{1}{n}\|\tilde{X}\Delta\|_2^2 \leq \frac{2}{n}(\tilde{y} - \tilde{X}\beta^*)^\top \tilde{X}\Delta + \lambda_1(\|\tilde{\Gamma}\beta^*\|_1 - \|\tilde{\Gamma}\hat{\beta}\|_1).$$

First we control the term $(\tilde{y} - \tilde{X}\beta^*)^\top \tilde{X}\Delta$. Using basic algebra,

$$(\tilde{y} - \tilde{X}\beta^*)^\top \tilde{X}\Delta = \epsilon^\top X\Delta - n\lambda_S\beta^{*\top}\Gamma^\top\Gamma\Delta.$$

Since $\tilde{\Gamma}^\dagger\tilde{\Gamma} = I_{p \times p}$, where $\tilde{\Gamma}^\dagger$ is the pseudo-inverse of $\tilde{\Gamma}$. Therefore

$$\begin{aligned} \epsilon^\top X\Delta &= \epsilon^\top X\tilde{\Gamma}^\dagger\tilde{\Gamma}\Delta \\ &\leq \|(X\tilde{\Gamma}^\dagger)^\top\epsilon\|_\infty\|\tilde{\Gamma}\Delta\|_1. \end{aligned}$$

To bound $n\lambda_S\beta^{*\top}\Gamma^\top\Gamma\Delta$ by

$$\begin{aligned} n\lambda_S\beta^{*\top}\Gamma^\top\Gamma\Delta &\leq n\lambda_S\|\Gamma^\top\Gamma\beta^*\|_\infty\|\Delta\|_1 \\ &\leq n\lambda_S\|L\beta^*\|_\infty\|\tilde{\Gamma}\Delta\|_1 \\ &\leq n\frac{\lambda_1}{8}\|\tilde{\Gamma}\Delta\|_1, \end{aligned}$$

where the last inequality follows from the constraint that $\lambda_1 \geq 8\lambda_S\|L\beta^*\|_\infty$. Now recall the constraint $\lambda_1 \geq 48\rho\sigma\sqrt{\frac{c_u \log p}{n}}$, the following lemma shows that with high probability we have $\lambda_1 \geq \frac{8}{n}\|(X\tilde{\Gamma}^\dagger)^\top\epsilon\|_\infty$.

Lemma 6. *Suppose we have $\lambda_1 \geq 48\rho\sigma\sqrt{\frac{c_u \log p}{n}}$. Then with probability at least $1 - \frac{C_1}{p}$,*

$$\lambda_1 \geq \frac{8}{n}\|(X\tilde{\Gamma}^\dagger)^\top\epsilon\|_\infty$$

for absolute constant $C_1 > 0$.

The proof of Lemma 6 is deferred to the Appendix. Combining the constraints for λ_1 with the inequalities above,

$$\frac{2}{n}(\tilde{y} - \tilde{X}\beta^*)^\top \tilde{X}\Delta \leq \frac{\lambda_1}{4}\|\tilde{\Gamma}\Delta\|_1 + \frac{\lambda_1}{4}\|\tilde{\Gamma}\Delta\|_1 = \frac{\lambda_1}{2}\|\tilde{\Gamma}\Delta\|_1.$$

Putting these pieces together we have

$$\frac{1}{n}\|\tilde{X}\Delta\|_2^2 \leq \frac{\lambda_1}{2}(\|\tilde{\Gamma}\Delta\|_1 + 2\|\tilde{\Gamma}\beta^*\|_1 - 2\|\tilde{\Gamma}\hat{\beta}\|_1). \quad (11)$$

Furthermore by the triangle inequality and the fact that $\frac{1}{n}\|\tilde{X}\Delta\|_2^2 \geq 0$ we have

$$0 \leq \|\tilde{\Gamma}(\hat{\beta} - \beta^*)\|_1 + 2\|\tilde{\Gamma}\beta^*\|_1 - 2\|\tilde{\Gamma}\hat{\beta}\|_1 \leq 3\|(\tilde{\Gamma}\Delta)_T\|_1 - \|(\tilde{\Gamma}\Delta)_{T^c}\|_1 + 4\|(\tilde{\Gamma}\beta^*)_{T^c}\|_1.$$

Therefore Δ lies in the translated cone

$$\mathcal{C} := \{v : \|(\tilde{\Gamma}v)_{T^c}\|_1 \leq 3\|(\tilde{\Gamma}v)_T\|_1 + 4\|(\tilde{\Gamma}\beta^*)_{T^c}\|_1\}. \quad (12)$$

Moreover by the definition of k_T we have

$$\|(\tilde{\Gamma}\Delta)_T\|_1 \leq \frac{\sqrt{|T|}\|\Delta\|_2}{k_T};$$

from (11) we have

$$\frac{1}{2n}\|\tilde{X}\Delta\|_2^2 \leq \lambda_1\|(\tilde{\Gamma}\beta^*)_{T^c}\|_1 + \frac{3\lambda_1}{4k_T}\sqrt{|T|}\|\Delta\|_2. \quad (13)$$

6.1.1. Restricted Eigenvalue Condition for \tilde{X}

From (11) and (12) we need to lower bound

$$\frac{\|\tilde{X}\Delta\|_2^2}{n} = \Delta^\top \left(\frac{X^\top X}{n} + \lambda_S L \right) \Delta,$$

for all Δ belonging to the cone \mathcal{C} defined in (12). The result is stated in the following lemma:

Lemma 7. *For all Δ belonging to the cone defined in (12) if we have*

$$\lambda_1 \leq c_2 \sqrt{\frac{\lambda_{\min}(\Sigma + \lambda_S L)}{|T|}} k_T, \quad (14)$$

then

$$\Delta^\top \left(\frac{X^\top X}{n} + \lambda_S L \right) \Delta \geq c_1 \lambda_{\min}(\Sigma + \lambda_S L) \|\Delta\|_2^2 - c_3 \lambda_1^2 \|(\tilde{\Gamma}\beta^*)_{T^c}\|_1^2 \quad (15)$$

holds with probability at least $1 - c_4 \exp(-c_5 n)$, where $c_i > 0$ for $i = 1, \dots, 5$ are positive constants.

The proof for this lemma is deferred to the Appendix and is based on the technique used in [Raskutti, Wainwright and Yu \(2010\)](#).

6.1.2. Final Part for Proof

From (13) and (15),

$$c_1 \lambda_{\min}(\Sigma + \lambda_S L) \|\Delta\|_2^2 - c_3 \lambda_1^2 \|(\tilde{\Gamma}\beta^*)_{T^c}\|_1^2 \leq 2\lambda_1 \|(\tilde{\Gamma}\beta^*)_{T^c}\|_1 + \frac{3\lambda_1}{2k_T} \sqrt{|T|} \|\Delta\|_2,$$

which is a quadratic inequality involving $\|\Delta\|_2$ as follows:

$$a \|\Delta\|_2^2 - b \|\Delta\|_2 - c \leq 0$$

with

$$\begin{aligned} a &= 1, \\ b &= \frac{3\lambda_1 \sqrt{|T|}}{2c_1 k_T \lambda_{\min}(\Sigma + \lambda_S L)}, \\ c &= \frac{1}{c_1 \lambda_{\min}(\Sigma + \lambda_S L)} (2\lambda_1 \|(\tilde{\Gamma}\beta^*)_{T^c}\|_1 + c_3 \lambda_1^2 \|(\tilde{\Gamma}\beta^*)_{T^c}\|_1^2). \end{aligned}$$

By solving this quadratic inequality,

$$\|\Delta\|_2^2 \leq 4 \max\{b^2, |c|\}.$$

Therefore there exists a positive constant C_u such that

$$\|\hat{\beta} - \beta^*\|_2^2 \leq C_u \max \left\{ \frac{\lambda_1^2 |T|}{k_T^2 \lambda_{\min}^2(\Sigma + \lambda_S L)}, \frac{\lambda_1 \|(\tilde{\Gamma}\beta^*)_{T^c}\|_1 + \lambda_1^2 \|(\tilde{\Gamma}\beta^*)_{T^c}\|_1^2}{\lambda_{\min}(\Sigma + \lambda_S L)} \right\}.$$

Note that the above inequality is true for all T , thus

$$\|\hat{\beta} - \beta^*\|_2^2 \leq C_u \min_T \max \left\{ \frac{\lambda_1^2 |T|}{k_T^2 \lambda_{\min}^2(\Sigma + \lambda_S L)}, \frac{\lambda_1 \|(\tilde{\Gamma}\beta^*)_{T^c}\|_1 + \lambda_1^2 \|(\tilde{\Gamma}\beta^*)_{T^c}\|_1^2}{\lambda_{\min}(\Sigma + \lambda_S L)} \right\}.$$

This completes the proof.

6.2. Proof of Theorem 2

The upper bound result $\|\hat{\beta} - \beta^*\|_2^2$ stated in Theorem 1 holds for all choices of T . If we choose $T = \text{supp}(\tilde{\Gamma}\beta^*)$ then $\|(\tilde{\Gamma}\beta^*)_{T^c}\|_1 = 0$ and by Lemma 2,

$$k_T^{-1} \leq \frac{\lambda_{\text{TV}} \sqrt{2\|\hat{\Sigma}\|_{1,1} \|\Gamma\beta^*\|_0 + \|\beta^*\|_0}}{\sqrt{\|\Gamma\beta^*\|_0 + \|\beta^*\|_0}}.$$

Then by Theorem 1 we have

$$\|\hat{\beta} - \beta^*\|_2^2 \leq \frac{2C_u}{\lambda_{\min}^2(\Sigma + \lambda_S L)} (\lambda_1^2 \|\beta^*\|_0 + 2\lambda_1^2 \lambda_{\text{TV}}^2 \|\hat{\Sigma}\|_{1,1} \|\Gamma\beta^*\|_0). \quad (16)$$

On the other hand if we choose $T = \text{supp}(\beta^*)$, $\|(\tilde{\Gamma}\beta^*)_{T^c}\|_1 = \lambda_{\text{TV}} \|\Gamma\beta^*\|_1$ and by Lemma 2, $k_T^{-1} \leq 1$. Thus if $\lambda_1 \lambda_{\text{TV}} \|\Gamma\beta^*\|_1 \leq 1$ by Theorem 1

$$\|\hat{\beta} - \beta^*\|_2^2 \leq C_u \left(\frac{\lambda_1^2 \|\beta^*\|_0}{\lambda_{\min}^2(\Sigma + \lambda_S L)} + \frac{2\lambda_1 \lambda_{\text{TV}} \|\Gamma\beta^*\|_1}{\lambda_{\min}(\Sigma + \lambda_S L)} \right). \quad (17)$$

Theorem 2 follows by combining (16) and (17) and taking the minimum over these two choices of T .

7. Conclusion

This paper describes a new graph-based regularization method for high-dimensional regression with highly-correlated designs. The structure of the estimator leverages ideas behind the Elastic Net (Zou and Hastie, 2005), the Fused LASSO (Tibshirani et al., 2005), the edge LASSO (Sharpnack, Singh and Rinaldo, 2012), trend filtering on graphs (Wang et al., 2016), and graph total variation (Shuman et al., 2013; Hütter and Rigollet, 2016). Unlike these past works, this paper explores how graph-based regularization can mitigate the effects of highly-correlated covariates. Under our model, the graph corresponding to the covariance structure of the covariates also provides prior information about the similarities among elements in the regression weights. Thus this graph allows us to effectively pre-condition our design matrix and regularize regression weights to promote alignment with the covariance structure of the problem. Hence we are able to provide mean-squared error bounds in settings where covariates are highly dependent, provided there is alignment between the β^* and graph. We also demonstrate through both simulations and an fMRI application superior performance of our compared to both OWL and Cluster LASSO. In addition, the proposed framework allows us to leverage correlation structure jointly with the response variable y , in contrast to previous work that depended upon clustering covariates independent of the responses. In settings where there exist very strong clusters (like the block graph studied above), clustering with and without responses yield similar results. However, when correlations are too weak to reveal strong clusters and yet too strong for the LASSO alone to be effective (like with the chain graph studied above), the implicit response-based clustering associated with our method can yield significant performance benefits. The results in this paper suggest several exciting avenues for future exploration, including more refined performance bounds for additional classes of graphs, extensions to logistic regression and other linear models, and more extensive evaluations on real-world data.

8. Appendix

8.1. Proof of Lemma 1

First note that

$$\begin{aligned}\lambda_{\min}(\Sigma + \lambda_S L) &= \lambda_{\min}((1 - \lambda_S)\Sigma + \lambda_S(\Sigma + L)) \\ &\geq (1 - \lambda_S)\lambda_{\min}(\Sigma) + \lambda_S\lambda_{\min}(\Sigma + L)\end{aligned}$$

where the second inequality follows from Weyl's inequality. For the remainder of the proof, we bound $\lambda_{\min}(\Sigma + L)$. Recall that

$$\Sigma + L = \Sigma - \hat{\Sigma} + D \tag{18}$$

where $D \in \mathbb{R}^{p \times p}$ is a diagonal matrix with

$$D_{jj} = \sum_{k=1}^p |\hat{\Sigma}_{j,k}|, \quad 1 \leq j \leq p.$$

Then

$$\lambda_{\min}(\Sigma + L) = \lambda_{\min}(\Sigma - \hat{\Sigma} + D) \geq \lambda_{\min}(\Sigma - \hat{\Sigma}) + \lambda_{\min}(D)$$

by Weyl's inequality. Since

$$\lambda_{\min}(\Sigma - \hat{\Sigma}) = -\lambda_{\max}(\hat{\Sigma} - \Sigma) \geq -\|\Sigma - \hat{\Sigma}\|_{op} \geq -\|\Sigma - \hat{\Sigma}\|_{1,1}.$$

Hence

$$\begin{aligned}
\lambda_{\min}(\Sigma + L) &\geq \lambda_{\min}(D) - \|\Sigma - \hat{\Sigma}\|_{1,1} \\
&\geq \min_j \sum_{k=1}^p |\hat{\Sigma}_{j,k}| - \frac{c_\ell}{4} \text{ (by Assumption 3.3)} \\
&\geq \min_j \left[\sum_{k=1}^p |\Sigma_{j,k}| - \sum_{k=1}^p |\Sigma_{j,k} - \hat{\Sigma}_{j,k}| \right] - \frac{c_\ell}{4} \\
&\geq \min_j \sum_{k=1}^p |\Sigma_{j,k}| - \max_j \sum_{k=1}^p |\Sigma_{j,k} - \hat{\Sigma}_{j,k}| - \frac{c_\ell}{4} \\
&\geq c_\ell - \frac{c_\ell}{4} - \frac{c_\ell}{4} = \frac{c_\ell}{2} \text{ (by Assumptions 3.2 and 3.3)}.
\end{aligned}$$

8.2. Proof of Lemma 2

By the definition of k_T we have

$$\begin{aligned}
\sqrt{|T|} k_T^{-1} &= \sup_{\beta} \frac{\|(\tilde{\Gamma}\beta)_T\|_1}{\|\beta\|_2} \\
&= \sup_{\beta: \|\beta\|_2=1} \|(\tilde{\Gamma}\beta)_T\|_1 \\
&= \sup_{\beta: \|\beta\|_2=1} \lambda_{\text{TV}} \|(\Gamma\beta)_{T_1}\|_1 + \|\beta_{T_2}\|_1 \\
&\leq \sup_{\beta: \|\beta\|_2=1} \lambda_{\text{TV}} \|(\Gamma\beta)_{T_1}\|_1 + \sqrt{|T_2|} \|\beta\|_2 \\
&\leq \sup_{\beta: \|\beta\|_2=1} \lambda_{\text{TV}} \|(\Gamma\beta)_{T_1}\|_1 + \sqrt{|T_2|}.
\end{aligned}$$

Next we will bound the term $\|(\Gamma\beta)_{T_1}\|_1$. First note that

$$\begin{aligned}
\|(\Gamma\beta)_{T_1}\|_1 &\leq \sqrt{|T_1|} \|(\Gamma\beta)_{T_1}\|_2 \\
&\leq \sqrt{|T_1| \sum_{(j,k) \in E \cap T_1} |\hat{\Sigma}_{j,k}| \|\beta_j - \text{sign}(\hat{\Sigma}_{j,k})\beta_k\|^2} \\
&\leq \sqrt{|T_1| \sum_{(j,k) \in E \cap T_1} |\hat{\Sigma}_{j,k}| (2|\beta_j|^2 + 2|\beta_k|^2)} \\
&\leq \sqrt{|T_1| \sum_{j=1}^p \left(\sum_{k: (j,k) \in E \cap T_1} 2|\hat{\Sigma}_{j,k}| \right) |\beta_j|^2} \\
&\leq \sqrt{|T_1|} \sqrt{\max_{1 \leq j \leq p} \left[\left(\sum_{k: (j,k) \in E \cap T_1} 2|\hat{\Sigma}_{j,k}| \right) \right]} \sqrt{\sum_{j=1}^p |\beta_j|^2} \\
&\leq \sqrt{|T_1|} \sqrt{\max_{1 \leq j \leq p} \left[\left(\sum_{k: (j,k) \in E \cap T_1} 2|\hat{\Sigma}_{j,k}| \right) \right]} \\
&\leq \sqrt{|T_1|} \sqrt{2\|\hat{\Sigma}\|_{1,1}}.
\end{aligned}$$

Thus

$$k_T^{-1} \leq \frac{\lambda_{\text{TV}} \sqrt{2\|\hat{\Sigma}\|_{1,1}|T_1|} + \sqrt{|T_2|}}{\sqrt{|T_1| + |T_2|}},$$

which completes the proof.

8.3. Proof of Lemma 3

Note that Γ is the edge incidence matrix and $L = \Gamma^\top \Gamma$ is the weighted graph Laplacian matrix. Let the singular value decomposition for Γ to be $\Gamma = U_{m \times p} D_{p \times p} V_{p \times p}^\top$. Next recall that $\tilde{\Gamma} = \begin{bmatrix} \lambda_{\text{TV}} \Gamma^\top \\ I \end{bmatrix}$, then we have

$$\begin{aligned} \tilde{\Gamma}^\dagger &= (\lambda_{\text{TV}}^2 \Gamma^\top \Gamma + I)^{-1} \begin{bmatrix} \lambda_{\text{TV}} \Gamma^\top & I \end{bmatrix} \\ &= (\lambda_{\text{TV}}^2 V D^2 V^\top + I)^{-1} \begin{bmatrix} \lambda_{\text{TV}} V D U^\top & I \end{bmatrix} \\ &= V (\lambda_{\text{TV}}^2 D^2 + I)^{-1} V^\top \begin{bmatrix} \lambda_{\text{TV}} V D U^\top & I \end{bmatrix} \\ &= \begin{bmatrix} \underbrace{V (\lambda_{\text{TV}}^2 D^2 + I)^{-1} \lambda_{\text{TV}} D U^\top}_{=:A} & \underbrace{V (\lambda_{\text{TV}}^2 D^2 + I)^{-1} V^\top}_{=:B} \end{bmatrix}. \end{aligned}$$

From the definition of ρ we can see that the maximum diagonal entry of $(\tilde{\Gamma}^\dagger)^\top \tilde{\Gamma}^\dagger$ will just be ρ^2 . Since

$$(\tilde{\Gamma}^\dagger)^\top \tilde{\Gamma}^\dagger = \begin{bmatrix} A^\top A & A^\top B \\ B^\top A & B^\top B \end{bmatrix},$$

we need to find the maximum diagonal values for matrices $A^\top A$ and $B^\top B$.

Suppose there are K connected components in the associated graph G . Thus the weighted graph Laplacian matrix L is block diagonal, as is the matrix V (after appropriate permutation of rows and columns), with each block corresponding to a different connected components. That is, each of the K connected components of the graph has its own weighted graph Laplacian $L_k = V_k D_k^2 V_k^\top$, for $k = 1, \dots, K$ and the diagonal blocks of V are the V_k s. Let μ_k be the minimum nonzero eigenvalue of L_k . Let B_k be the subset of vertices in the k -th connected component and $|B_k|$ be the number of vertices in that component, and let $k(i)$ denote which block contains vertex i . Now let v_i^\top be the i -th row of V , u_i^\top be the i -th row of U , and note that v_i is only supported on $B_{k(i)}$. Further note that the first (upper left) element of the k -th diagonal block of V is $1/\sqrt{|B_k|}$ if the minimum eigenvalue of L_k is 0. Then we have:

$$B^\top B = V (\lambda_{\text{TV}}^2 D^2 + I)^{-2} V^\top,$$

and then the maximum diagonal element for $B^\top B$ can be upper bounded as:

$$\begin{aligned} \max \text{diag}(B^\top B) &= \max_{i \in \{1, \dots, p\}} v_i^\top (\lambda_{\text{TV}}^2 D^2 + I)^{-2} v_i \\ &= \max_{i \in \{1, \dots, p\}} \sum_{j=1}^p \frac{v_{j,i}^2}{(\lambda_{\text{TV}}^2 D_{jj}^2 + 1)^2} \\ &= \max_{i \in \{1, \dots, p\}} \sum_{j \in B_{k(i)}} \frac{v_{j,i}^2}{(\lambda_{\text{TV}}^2 D_{jj}^2 + 1)^2} \\ &\leq \max_{i \in \{1, \dots, p\}} \left\{ \frac{1}{|B_{k(i)}|} + \sum_{\substack{j \in B_{k(i)} \\ D_{jj}^2 > 0}} \frac{v_{j,i}^2}{(\lambda_{\text{TV}}^2 D_{jj}^2 + 1)^2} \right\} \\ &\leq \max_{i \in \{1, \dots, p\}} \left\{ \frac{1}{|B_{k(i)}|} + \frac{1}{(\lambda_{\text{TV}}^2 \mu_{k(i)} + 1)^2} \sum_{\substack{j \in B_{k(i)} \\ D_{jj}^2 > 0}} v_{j,i}^2 \right\} \\ &\leq \max_{i \in \{1, \dots, p\}} \left\{ \frac{1}{|B_{k(i)}|} + \frac{1}{(\lambda_{\text{TV}}^2 \mu_{k(i)} + 1)^2} \right\} \\ &\leq \max_{k \in \{1, \dots, K\}} \left\{ \frac{1}{|B_k|} + \frac{1}{(\lambda_{\text{TV}}^2 \mu_k + 1)^2} \right\}. \end{aligned}$$

On the other hand we note that

$$A^\top A = U \lambda_{\text{TV}}^2 D^2 (\lambda_{\text{TV}}^2 D^2 + I)^{-2} U^\top,$$

similarly the maximum diagonal element for $A^\top A$ can be upper bounded as:

$$\begin{aligned} \max \text{diag}(A^\top A) &= \max_{i \in \{1, \dots, m\}} u_i^\top \lambda_{\text{TV}}^2 D^2 (\lambda_{\text{TV}}^2 D^2 + I)^{-2} u_i \\ &= \max_{i \in \{1, \dots, m\}} \sum_{j=1}^p \frac{\lambda_{\text{TV}}^2 D_{jj}^2 u_{j,i}^2}{(\lambda_{\text{TV}}^2 D_{jj}^2 + 1)^2} \\ &= \max_{i \in \{1, \dots, m\}} \sum_{j=1}^p \frac{(\lambda_{\text{TV}}^2 D_{jj}^2 + 1 - 1) u_{j,i}^2}{(\lambda_{\text{TV}}^2 D_{jj}^2 + 1)^2} \\ &= \max_{i \in \{1, \dots, m\}} \sum_{j=1}^p \left\{ \frac{u_{j,i}^2}{\lambda_{\text{TV}}^2 D_{jj}^2 + 1} - \frac{u_{j,i}^2}{(\lambda_{\text{TV}}^2 D_{jj}^2 + 1)^2} \right\} \\ &\leq \max_{i \in \{1, \dots, m\}} \sum_{j \in \{1, \dots, p\}: D_{jj}^2 > 0} \left\{ \frac{u_{j,i}^2}{\lambda_{\text{TV}}^2 D_{jj}^2 + 1} \right\} \\ &\leq \max_{i \in \{1, \dots, m\}} \max_{j \in \{1, \dots, p\}: D_{jj}^2 > 0} \frac{1}{\lambda_{\text{TV}}^2 D_{jj}^2 + 1} \sum_{j=1}^p u_{j,i}^2 \\ &\leq \max_{i \in \{1, \dots, m\}} \max_{j \in \{1, \dots, p\}: D_{jj}^2 > 0} \frac{1}{\lambda_{\text{TV}}^2 D_{jj}^2 + 1} \\ &\leq \max_{k \in \{1, \dots, K\}} \frac{1}{\lambda_{\text{TV}}^2 \mu_k + 1}. \end{aligned}$$

Then by combining the results above we have

$$\begin{aligned} \rho^2 &\leq \max_{1 \leq k \leq K} \left\{ \frac{1}{|B_k|} + \frac{1}{(\lambda_{\text{TV}}^2 \mu_k + 1)^2} + \frac{1}{\lambda_{\text{TV}}^2 \mu_k + 1} \right\} \\ &\leq \max_{1 \leq k \leq K} \left\{ \frac{1}{|B_k|} + \frac{2}{\lambda_{\text{TV}}^2 \mu_k + 1} \right\}. \end{aligned}$$

This completes the proof of Lemma 3.

8.4. Proof of Lemma 4

By the definition for block complete graph in Section 3.2.1 we can see that $|B_k| = \frac{p}{K}$ for $1 \leq k \leq K$ thus we have $\max_{1 \leq k \leq K} \frac{1}{|B_k|} = \frac{K}{p}$. Note that μ_k is defined to be the smallest non-zero eigenvalue of weighted graph Laplacian matrix for the k^{th} complete graph. It is known that the smallest non-zero eigenvalue for un-weighted Laplacian matrix for complete graph is the number of nodes (see Hütter and Rigollet (2016, Section 4.1)). Thus, applying appropriate normalization $\mu_k = ar|B_k| = ar \frac{p}{K} = r$ since $a = \frac{K}{p}$. Hence $\mu_k = r$ for $1 \leq k \leq K$. Also note that $\lambda_{\min}(\Sigma) = a(1 - r)$, then we have

$$\begin{aligned} \lambda_{\min}(\Sigma + \lambda_S L) &= \lambda_{\min}[(1 - \lambda_S)\Sigma + \lambda_S(\Sigma + L)] \\ &\geq (1 - \lambda_S)\lambda_{\min}(\Sigma) + \lambda_S \lambda_{\min}(\Sigma + L) \\ &= (1 - \lambda_S)a(1 - r) + \lambda_S[a + ar(\frac{p}{K} - 1)] \text{ (by (18) and } \hat{\Sigma} = \Sigma) \\ &\geq (1 - \lambda_S)(1 - r)\frac{K}{p} + \lambda_S r \text{ (by using } a = \frac{K}{p}). \end{aligned}$$

This completes the proof of Lemma 4.

8.5. Proof of Lemma 5

First from the definition of chain graph in Section 3.2.2 we know there is only one connected component B_1 , thus $\frac{1}{|B_1|} = \frac{1}{p}$. The smallest non-zero eigenvalue for un-weighted Laplacian matrix for chain graph with size p equals $2 - 2 \cos(\frac{\pi}{p})$ (see Hütter and Rigollet (2016, Section B.2)). Then by the definition of μ_1 we have $\mu_1 = (2 - 2 \cos(\frac{\pi}{p}))ar = (2 - 2 \cos(\frac{\pi}{p}))r$ since $a = 1$. Also note that $\lambda_{\min}(\Sigma) = a[1 + 2r \cos(\frac{p}{p+1}\pi)]$ (see Noschese, Pasquini and Reichel (2013, Section 2)), then we have

$$\begin{aligned} \lambda_{\min}(\Sigma + \lambda_S L) &= \lambda_{\min}[(1 - \lambda_S)\Sigma + \lambda_S(\Sigma + L)] \\ &\geq (1 - \lambda_S)\lambda_{\min}(\Sigma) + \lambda_S\lambda_{\min}(\Sigma + L) \\ &= (1 - \lambda_S)a[1 + 2r \cos(\frac{p}{p+1}\pi)] + \lambda_S a(1 + r) \text{ (by (18) and } \hat{\Sigma} = \Sigma) \\ &\geq (1 - \lambda_S)[1 + 2r \cos(\frac{p}{p+1}\pi)] + \lambda_S \text{ (by using } a = 1) \\ &\geq (1 - \lambda_S)(1 - 2r) + \lambda_S. \end{aligned}$$

This completes the proof of Lemma 5.

8.6. Proof of Lemma 6

We will use two classical Lemmas for Gaussian processes Anderson (1984); Slepian (1962) to prove our results.

Lemma 8 (Anderson's comparison inequality). *Let X and Y be zero-mean Gaussian random vectors with covariance Σ_X and Σ_Y respectively. If $\Sigma_Y - \Sigma_X$ is positive semi-definite then for any convex symmetric set C ,*

$$P(X \in C) \leq P(Y \in C).$$

Lemma 9 (Slepian's Lemma). *Let $\{G_s, s \in S\}$ and $\{H_s, s \in S\}$ be two centered Gaussian processes defined over the same index set S . Suppose that both processes are almost surely bounded. For each $s, t \in S$, if $\mathbb{E}(G_s - G_t)^2 \leq \mathbb{E}(H_s - H_t)^2$, then $\mathbb{E}[\sup_{s \in S} G_s] \leq \mathbb{E}[\sup_{s \in S} H_s]$. Further if $\mathbb{E}(G_s^2) = \mathbb{E}(H_s^2)$ for all $s \in S$, then*

$$P\{\sup_{s \in S} G_s > x\} \leq P\{\sup_{s \in S} H_s > x\},$$

for all $x > 0$.

$(X\tilde{\Gamma}^\dagger)^\top \epsilon = \sum_{i=1}^n \langle \tilde{\Gamma}^\dagger, \epsilon_i X^{(i)} \rangle$ and $Cov(X) = \Sigma \preceq \lambda_{\max}(\Sigma)I_{p \times p}$. Then by Assumption 3.1 $\lambda_{\max}(\Sigma) \leq c_u$, and if we use Lemma 8, for any $x > 0$

$$P\{\sup \sum_{i=1}^n \langle \tilde{\Gamma}^\dagger, \epsilon_i X^{(i)} \rangle \leq x\} \geq P\{\sup \sqrt{c_u} \sum_{i=1}^n \langle \tilde{\Gamma}^\dagger, \epsilon_i g_i \rangle \leq x\},$$

where $X^{(i)}$ is the i^{th} row of matrix X and $\{g_i : i = 1, \dots, n\}$ is i.i.d. standard normal Gaussian vectors with $g_i \in \mathbb{R}^p$. Now let $G \in \mathbb{R}^p$ be an i.i.d. standard norm Gaussian vector and define the zero-mean Gaussian process $\sqrt{n}\sigma \langle \tilde{\Gamma}^\dagger, G \rangle$, we can see that the conditions in Lemma 9 are satisfied for two centered Gaussian processes $\sum_{i=1}^n \langle \tilde{\Gamma}^\dagger, \epsilon_i g_i \rangle$ and $\sqrt{n}\sigma \langle \tilde{\Gamma}^\dagger, G \rangle$ thus we have

$$P\{\sup \sqrt{c_u} \sum_{i=1}^n \langle \tilde{\Gamma}^\dagger, \epsilon_i g_i \rangle \leq x\} \geq P\{\sup \sigma \sqrt{nc_u} \langle \tilde{\Gamma}^\dagger, G \rangle \leq x\}.$$

Further, using known results on Gaussian maxima (Boucheron, Lugosi and Massart (2013, Theorem 2.5)), $\sup \langle \tilde{\Gamma}^\dagger, G \rangle \leq 3\rho\sqrt{\log(m+p)}$ with probability at least $1 - \frac{C_1}{p}$ for some absolute constant $C_1 > 0$. By choosing $x = 3\sigma\rho\sqrt{nc_u \log(m+p)}$,

$$P\left\{\sup \sum_{i=1}^n \langle \tilde{\Gamma}^\dagger, \epsilon_i X^{(i)} \rangle \leq x\right\} \geq P\left\{\sup \sigma\sqrt{nc_u} \langle \tilde{\Gamma}^\dagger, G \rangle \leq x\right\} \geq 1 - \frac{C_1}{p}.$$

Thus we have shown with high probability that $\|(X\tilde{\Gamma}^\dagger)^\top \epsilon\|_\infty \leq 3\sigma\rho\sqrt{nc_u \log(m+p)}$. Since m is the number of edges, $m \leq \frac{p(p-1)}{2}$, thus with probability at least $1 - \frac{C_1}{p}$ we have that $\|(X\tilde{\Gamma}^\dagger)^\top \epsilon\|_\infty \leq 6\sigma\rho\sqrt{nc_u \log p}$. This completes the proof.

8.7. Proof of Lemma 7

The proof of Lemma 7 involves two parts.

Part 1: We first show that the following inequality

$$\frac{\|X\Delta\|_2}{\sqrt{n}} \geq \frac{1}{4}\|\Sigma^{1/2}\Delta\|_2 - 9\frac{\lambda_1}{\sigma}\|\tilde{\Gamma}\Delta\|_1 \quad (19)$$

holds with probability at least $1 - c_4 \exp(-c_5 n)$ by using similar techniques to those used to prove Theorem 1 in Raskutti, Wainwright and Yu (2010).

First note that it is sufficient to show (19) holds with $\|\Sigma^{1/2}\Delta\|_2 = 1$. The reason is as follows: if $\|\Sigma^{1/2}\Delta\|_2 = 0$ we can see that (19) holds trivially; otherwise when $\|\Sigma^{1/2}\Delta\|_2 > 0$ we can define $\tilde{\Delta} = \frac{\Delta}{\|\Sigma^{1/2}\Delta\|_2}$ then we have $\|\Sigma^{1/2}\tilde{\Delta}\|_2 = 1$. Since (19) is invariant with respect to the scale of Δ , if it holds for $\tilde{\Delta}$, it also holds for Δ . Thus in the following proof we just assume that $\|\Sigma^{1/2}\Delta\|_2 = 1$. To show (19) with $\|\Sigma^{1/2}\Delta\|_2 = 1$ holds there are three main steps:

(1) Since we want to lower bound $\frac{\|X\Delta\|_2}{\sqrt{n}}$ in terms of $\|\Sigma^{1/2}\Delta\|_2$ and $\|\tilde{\Gamma}\Delta\|_1$, we define the set $V(r) := \{\Delta \in \mathbb{R}^p \mid \|\Sigma^{1/2}\Delta\|_2 = 1, \|\tilde{\Gamma}\Delta\|_1 \leq r\}$ for a fixed radius r . Note that we are only concerned with choices of r such the set $V(r)$ is non-empty. Our first step is to give an upper bound for $\mathbb{E}[M(r, X)]$, where $M(r, X)$ is defined as:

$$M(r, X) := 1 - \inf_{\Delta \in V(r)} \frac{\|X\Delta\|_2}{\sqrt{n}} = \sup_{\Delta \in V(r)} \left\{ 1 - \frac{\|X\Delta\|_2}{\sqrt{n}} \right\}.$$

(2) The second step is to use concentration inequalities to show that with high probability for each fixed $r > 0$, the random quantity $M(r, X)$ is sharply concentrated around $\mathbb{E}[M(r, X)]$.

(3) The third step is to use a peeling argument to show that the analysis holds uniformly over all possible values of r with high probability, then we can show that (19) holds with high probability.

In the following proof we only provide details for proving step (1) since our proof for step (2) and (3) will be identical to those in Raskutti, Wainwright and Yu (2010). For step (1) we prove the following lemma:

Lemma 10. *For any radius $r > 0$ such that $V(r)$ is non-empty, we have*

$$\mathbb{E}[M(r, X)] \leq \frac{1}{4} + 3r\frac{\lambda_1}{\sigma}.$$

Proof. Define the Euclidean sphere of radius 1 to be $S^{n-1} = \{u \in \mathbb{R}^n \mid \|u\|_2 = 1\}$. Then $\|X\Delta\|_2 = \sup_{u \in S^{n-1}} u^\top X\Delta$. In order to write the quantity $M(r, X)$ in a form that is easier to analyze, we define $Y_{u,\Delta} := u^\top X\Delta$ for each pair $(u, \Delta) \in S^{n-1} \times V(r)$. Then we have

$$- \inf_{\Delta \in V(r)} \|X\Delta\|_2 = - \inf_{\Delta \in V(r)} \sup_{u \in S^{n-1}} u^\top X\Delta = \sup_{\Delta \in V(r)} \inf_{u \in S^{n-1}} Y_{u,\Delta}.$$

Next we will use a Gaussian comparison inequality to upper bound the expected value of the quantity $\sup_{\Delta \in V(r)} \inf_{u \in S^{n-1}} Y_{u,\Delta}$. Here we use a form of Gordon's inequality that is stated in [Davidson and Szarek \(2001\)](#) for our analysis. Suppose that $\{Y_{u,\Delta}, (u, \Delta) \in U \times V\}$ and $\{Z_{u,\Delta}, (u, \Delta) \in U \times V\}$ are two zero-mean Gaussian processes on $U \times V$. We denote $\sigma(\cdot)$ to be the standard deviation of a random variable. Using Gordon's inequality, if

$$\sigma(Y_{u,\Delta} - Y_{u',\Delta'}) \leq \sigma(Z_{u,\Delta} - Z_{u',\Delta'}), \quad \forall (u, \Delta) \text{ and } (u', \Delta') \in U \times V,$$

and this inequality holds with equality when $\Delta = \Delta'$, then

$$\mathbb{E}[\sup_{\Delta \in V} \inf_{u \in U} Y_{u,\Delta}] \leq \mathbb{E}[\sup_{\Delta \in V} \inf_{u \in U} Z_{u,\Delta}].$$

Now we consider the zero-mean Gaussian process $Z_{u,\Delta}$ with $(u, \Delta) \in S^{n-1} \times V(r)$ as follows:

$$Z_{u,\Delta} = g^\top u + h^\top \Sigma^{1/2} \Delta,$$

where $g \sim \mathcal{N}(0, I_{n \times n})$ and $h \sim \mathcal{N}(0, I_{p \times p})$. It follows that (see [Raskutti, Wainwright and Yu \(2010\)](#) for more details)

$$\sigma(Y_{u,\Delta} - Y_{u',\Delta'}) \leq \sigma(Z_{u,\Delta} - Z_{u',\Delta'}), \quad \forall (u, \Delta) \text{ and } (u', \Delta') \in S^{n-1} \times V(r),$$

and the equality holds when $\Delta = \Delta'$. Thus we can apply Gordon's inequality to conclude that

$$\begin{aligned} \mathbb{E}[\sup_{\Delta \in V(r)} \inf_{u \in S^{n-1}} Y_{u,\Delta}] &\leq \mathbb{E}[\sup_{\Delta \in V(r)} \inf_{u \in S^{n-1}} Z_{u,\Delta}] \\ &= \mathbb{E}[\inf_{u \in S^{n-1}} g^\top u] + \mathbb{E}[\sup_{\Delta \in V(r)} h^\top \Sigma^{1/2} \Delta] \\ &= -\mathbb{E}[\|g\|_2] + \mathbb{E}[\sup_{\Delta \in V(r)} h^\top \Sigma^{1/2} \Delta]. \end{aligned}$$

Next we bound the term $\mathbb{E}[\sup_{\Delta \in V(r)} h^\top \Sigma^{1/2} \Delta]$ using the following lemma:

Lemma 11. *Suppose we have $\lambda_1 \geq 48\rho\sigma\sqrt{\frac{c_u \log p}{n}}$, then we have that*

$$\lambda_1 \geq 8 \frac{\sigma}{\sqrt{n}} \mathbb{E}[\|(\Sigma^{1/2} \tilde{\Gamma}^\dagger)^\top h\|_\infty].$$

with high probability at least $1 - \frac{c}{p}$ for some absolute constant $c > 0$.

The proof for this lemma will be provided shortly. Thus

$$\begin{aligned} \mathbb{E}[\sup_{\Delta \in V(r)} |h^\top \Sigma^{1/2} \Delta|] &= \mathbb{E}[\sup_{\Delta \in V(r)} |h^\top \Sigma^{1/2} \tilde{\Gamma}^\dagger \tilde{\Gamma} \Delta|] \\ &\leq \mathbb{E}[\sup_{\Delta \in V(r)} \|h^\top \Sigma^{1/2} \tilde{\Gamma}^\dagger\|_\infty \|\tilde{\Gamma} \Delta\|_1] \\ &\leq \mathbb{E}[\|(\Sigma^{1/2} \tilde{\Gamma}^\dagger)^\top h\|_\infty] r \\ &\leq 3r \frac{\lambda_1}{\sigma} \sqrt{n}, \end{aligned}$$

where the last inequality holds with high probability from Lemma 11. Also by standard χ^2 tail bounds (Ledoux and Talagrand, 1991) when $n \geq 10$ we have $\mathbb{E}[\|g\|_2] \geq \frac{3}{4}\sqrt{n}$. By combining these pieces together

$$\mathbb{E}\left[-\inf_{\Delta \in V(r)} \|X\Delta\|_2\right] \leq -\frac{3}{4}\sqrt{n} + 3r\frac{\lambda_1}{\sigma}\sqrt{n}.$$

Thus by dividing by \sqrt{n} and adding 1 to both sides we have

$$\mathbb{E}[M(r, X)] = \mathbb{E}\left[1 - \inf_{\Delta \in V(r)} \frac{\|X\Delta\|_2}{\sqrt{n}}\right] \leq \frac{1}{4} + 3r\frac{\lambda_1}{\sigma}.$$

□

Then by following the rest proof in Raskutti, Wainwright and Yu (2010) for step (2) and (3), we can show that with probability at least $1 - c_4 \exp(-c_5 n)$,

$$\frac{\|X\Delta\|_2}{\sqrt{n}} \geq \frac{1}{4}\|\Sigma^{1/2}\Delta\|_2 - 9\frac{\lambda_1}{\sigma}\|\tilde{\Gamma}\Delta\|_1.$$

Part 2: Next we can go to second part of the proof. From (11) and (12) we know that

$$\begin{aligned} \|\tilde{\Gamma}\Delta\|_1 &\leq 4\|(\tilde{\Gamma}\Delta)_T\|_1 + 4\|(\tilde{\Gamma}\beta^*)_{T^c}\|_1 \\ &\leq \frac{4\sqrt{|T|}\|\Delta\|_2}{k_T} + 4\|(\tilde{\Gamma}\beta^*)_{T^c}\|_1. \end{aligned}$$

Then

$$\frac{\|X\Delta\|_2}{\sqrt{n}} \geq \frac{1}{4}\|\Sigma^{1/2}\Delta\|_2 - 9\frac{\lambda_1}{\sigma} \left(4\|(\tilde{\Gamma}\beta^*)_{T^c}\|_1 + \frac{4\sqrt{|T|}\|\Delta\|_2}{k_T} \right).$$

Thus there exist constants $c', c'' > 0$ such that

$$\Delta^\top \left(\frac{X^\top X}{n} + \lambda_S L \right) \Delta \geq c' \Delta^\top (\Sigma + \lambda_S L) \Delta - c'' \lambda_1^2 \left(\|(\tilde{\Gamma}\beta^*)_{T^c}\|_1^2 + \frac{|T|\|\Delta\|_2^2}{k_T^2} \right).$$

Since

$$\Delta^\top (\Sigma + \lambda_S L) \Delta \geq \lambda_{\min}(\Sigma + \lambda_S L) \|\Delta\|_2^2,$$

then when λ_1 satisfies (14) for some constant $c_2 > 0$,

$$\Delta^\top \left(\frac{X^\top X}{n} + \lambda_S L \right) \Delta \geq c_1 \lambda_{\min}(\Sigma + \lambda_S L) \|\Delta\|_2^2 - c_3 \lambda_1^2 \|(\tilde{\Gamma}\beta^*)_{T^c}\|_1^2,$$

for absolute constants $c_1, c_3 > 0$.

8.8. Proof of Lemma 11

Here we use similar techniques to the proof of Lemma 6. First note that $\Sigma \preceq c_u I_{p \times p}$ and by using Lemma 8 we have for any $y > 0$ the following inequality

$$P\{\sup[(\Sigma^{1/2}\tilde{\Gamma}^\dagger)^\top h] \leq y\} = P\{\sup\langle \tilde{\Gamma}^\dagger, \Sigma^{1/2}h \rangle \leq y\} \geq P\{\sup\langle \tilde{\Gamma}^\dagger, h \rangle \leq \frac{y}{\sqrt{c_u}}\}.$$

Since $h \sim \mathcal{N}(0, I_{p \times p})$ then also by known results on Gaussian maxima (Boucheron, Lugosi and Massart (2013, Theorem 2.5)) we have $\sup \langle \tilde{\Gamma}^\dagger, h \rangle \leq 3\rho\sqrt{\log(m+p)}$ with probability at least $1 - \frac{c}{p}$ for some constant $c > 0$. Then we can choose $y = 3\rho\sqrt{c_u \log(m+p)}$ and

$$P\{\sup[(\Sigma^{1/2}\tilde{\Gamma}^\dagger)^\top h] \leq y\} \geq P\{\sup \langle \tilde{\Gamma}^\dagger, h \rangle \leq \frac{y}{\sqrt{c_u}}\} \geq 1 - \frac{c}{p}.$$

Thus with high probability $\mathbb{E}[\|(\Sigma^{1/2}\tilde{\Gamma}^\dagger)^\top h\|_\infty] \leq 3\rho\sqrt{c_u \log(m+p)}$, then using the fact that $m \leq \frac{p(p-1)}{2}$, $\mathbb{E}[\|(\Sigma^{1/2}\tilde{\Gamma}^\dagger)^\top h\|_\infty] \leq 6\rho\sqrt{c_u \log p}$ holds with probability at least $1 - \frac{c}{p}$. This completes the proof of Lemma 11.

References

- ANDERSON, T. W. (1984). *An Introduction to Multivariate Statistical Analysis*. Wiley Series in Probability and Mathematical Statistics. Wiley, New York.
- BAIK, J. and SILVERSTEIN, J. W. (2006). Eigenvalues of large sample covariance matrices of spiked populations models. *Journal of Multivariate Analysis* **97** 1382–1408.
- BICKEL, P. and LEVINA, E. (2008a). Regularized estimation of large covariance matrices. *The Annals of Statistics* **36** 199–227.
- BICKEL, P. and LEVINA, E. (2008b). Covariance estimation by thresholding. *The Annals of Statistics* **36** 2577–2604.
- BICKEL, P., RITOV, Y. and TSYBAKOV, A. (2009). Simultaneous Analysis of Lasso and Dantzig Selector. *The Annals of Statistics* **37** 1705–1732.
- BONDELL, H. D. and REICH, B. J. (2008). Simultaneous regression shrinkage, variable selection, and supervised clustering of predictors with OSCAR. *Biometrics* **64** 115–123.
- BOUCHERON, S., LUGOSI, G. and MASSART, P. (2013). *Concentration inequalities: A nonasymptotic theory of independence*. Oxford university press.
- BÜHLMANN, P., RÜTIMANN, P., VAN DE GEER, S. and ZHANG, C. (2013). Correlated variables in regression: clustering and sparse estimation. *Journal of Statistical Planning and Inference* **143** 1835–1858.
- CAI, T. T. and LIU, W. (2011). Adaptive thresholding for sparse covariance matrix estimation. *Journal of the American Statistical Association* **106** 672–684.
- CAI, T. T., ZHAO, R. and ZHOU, H. H. (2016). Estimating structured high-dimensional covariance and precision matrices: Optimal rates and adaptive estimation. *Electron. J. Statist.* **10** 1–59.
- CANDES, E. J. and TAO, T. (2005). Decoding by linear programming. *IEEE transactions on information theory* **51** 4203–4215.
- DAVIDSON, K. R. and SZAREK, S. J. (2001). Local operator theory, random matrices, and Banach spaces. In *Handbook of Banach Spaces*, **1** 317–336. Elsevier, Amsterdam, NL.
- DAYE, Z. and JENG, X. (2009). Shrinkage and model selection with correlated variables via weighted fusion. *Computational Statistics & Data Analysis* **53** 1284–1298.
- DONOHO, D. L., GAVISH, M. and JOHNSTONE, I. M. (2013). Optimal shrinkage of eigenvalues in the spiked covariance model. *arXiv preprint arXiv:1311.0851*.
- FIGUEIREDO, M. and NOWAK, R. (2016). Ordered Weighted ℓ_1 Regularized Regression with Strongly Correlated Covariates: Theoretical Aspects. In *Proceedings of the 19th International Conference on Artificial Intelligence and Statistics* 930–938.
- GROSENICK, L., KLINGENBERG, B., GREER, S., TAYLOR, J. and KNUTSON, B. (2009). Whole-brain sparse penalized discriminant analysis for predicting choice. *NeuroImage* **47** S58.
- GROSENICK, L., KLINGENBERG, B., KNUTSON, B. and TAYLOR, J. (2011). A family of interpretable multivariate models for regression and classification of whole-brain fMRI data. *ArXiv e-prints* **1110**.

- HALLAC, D., LESKOVEC, J. and BOYD, S. (2015). Network lasso: Clustering and optimization in large graphs. In *Proceedings of the 21th ACM SIGKDD international conference on knowledge discovery and data mining* 387–396. ACM.
- HASTIE, T., TIBSHIRANI, R. and WAINWRIGHT, M. (2015). *Statistical learning with sparsity: the lasso and generalizations*. CRC press.
- HEBIRI, M. and VAN DE GEER, S. (2011). The Smooth-Lasso and other $\ell_1+\ell_2$ -penalized methods. *Electronic Journal of Statistics* **5** 1184–1226.
- HUANG, J., MA, S., LI, H. and ZHANG, C.-H. (2011). The sparse Laplacian shrinkage estimator for high-dimensional regression. *Ann. Statist.* **39** 2021–2046.
- HÜTTER, J. and RIGOLLET, P. (2016). Optimal rates for total variation denoising. *arXiv preprint arXiv:1603.09388*.
- JALALI, A. and FAZEL, M. (2013). A convex method for learning d-valued models. In *Global Conference on Signal and Information Processing (GlobalSIP), 2013 IEEE* 1123–1126. IEEE.
- JIA, J., ROHE, K. et al. (2015). Preconditioning the Lasso for sign consistency. *Electronic Journal of Statistics* **9** 1150–1172.
- LEDoux, M. and TALAGRAND, M. (1991). *Probability in Banach Spaces: Isoperimetry and Processes*. Springer-Verlag, New York, NY.
- LEWIS-PEACOCK, J. A. and POSTLE, B. R. (2008). Temporary activation of long-term memory supports working memory. *Journal of Neuroscience* **28** 8765–8771.
- LIU, J., YUAN, L. and YE, J. (2013). Dictionary LASSO: Guaranteed Sparse Recovery under Linear Transformation. *arXiv preprint arXiv:1305.0047*.
- MICHEL, V., GRAMFORT, A., VAROQUAUX, G., EGER, E. and THIRION, B. (2011). Total variation regularization for fMRI-based prediction of behavior. *IEEE transactions on medical imaging* **30** 1328–1340.
- NEEDEL, D. and WARD, R. (2013a). Stable image reconstruction using total variation minimization. *SIAM Journal on Imaging Sciences* **6** 1035–1058.
- NEEDEL, D. and WARD, R. (2013b). Near-optimal compressed sensing guarantees for total variation minimization. *IEEE Transactions on Image Processing* **22** 3941–3949.
- NEGAHBAN, S., RAVIKUMAR, P., WAINWRIGHT, M. J. and YU, B. (2012). A unified framework for high-dimensional analysis of M -estimators with decomposable regularizers. *Statistical Science* **27** 538–557.
- NOSCHESSE, S., PASQUINI, L. and REICHEL, L. (2013). Tridiagonal Toeplitz matrices: properties and novel applications. *Numerical linear algebra with applications* **20** 302–326.
- PRIM, R. C. (1957). Shortest connection networks and some generalizations. *Bell Labs Technical Journal* **36** 1389–1401.
- RASKUTTI, G., WAINWRIGHT, M. J. and YU, B. (2010). Restricted eigenvalue conditions for correlated Gaussian designs. *Journal of Machine Learning Research* **11** 2241–2259.
- RASKUTTI, G. and YUAN, M. (2015). Convex regularization for high-dimensional tensor regression. *arXiv preprint arXiv:1512.01215*.
- SADHANALA, V., WANG, Y. and TIBSHIRANI, R. (2016). Total variation classes beyond 1d: Minimax rates, and the limitations of linear smoothers. In *Advances in Neural Information Processing Systems* 3513–3521.
- SAUNDERSON, J., CHANDRASEKARAN, V., PARRILO, P. and WILLSKY, A. (2012). Diagonal and low-rank matrix decompositions, correlation matrices, and ellipsoid fitting. *SIAM Journal on Matrix Analysis and Applications* **33** 1395–1416.
- SHARMA, D. B., BONDELL, H. D. and ZHANG, H. H. (2013). Consistent Group Identification and Variable Selection in Regression With Correlated Predictors. *Journal of Computational and Graphical Statistics* **22** 319–340.

- SHARPNACK, J., SINGH, A. and RINALDO, A. (2012). Sparsistency of the edge lasso over graphs. In *Artificial Intelligence and Statistics* 1028–1036.
- SHE, Y. (2010). Sparse regression with exact clustering. *Electronic Journal of Statistics* **4** 1055–1096.
- SHEN, X. and HUANG, H.-C. (2010). Grouping pursuit through a regularization solution surface. *Journal of the American Statistical Association* **105** 727–739.
- SHEN, X., HUANG, H.-C. and PAN, W. (2012). Simultaneous supervised clustering and feature selection over a graph. *Biometrika* **99** 899–914.
- SHUMAN, D. I., NARANG, S. K., FROSSARD, P., ORTEGA, A. and VANDERGHEYNST, P. (2013). The emerging field of signal processing on graphs: Extending high-dimensional data analysis to networks and other irregular domains. *IEEE Signal Processing Magazine* **30** 83–98.
- SLEPIAN, D. (1962). The one-sided barrier problem for Gaussian noise. *Bell System Tech. J* **41** 463–501.
- TIBSHIRANI, R. (1996). Regression shrinkage and selection via the lasso. *Journal of the Royal Statistical Society, Series B* **58** 267–288.
- TIBSHIRANI, R. and TAYLOR, J. (2011). The solution path of the generalized lasso. *The Annals of Statistics* **39** 1335–1371.
- TIBSHIRANI, R., SAUNDERS, M., ROSSET, S., ZHU, J. and KNIGHT, K. (2005). Sparsity and smoothness via the fused lasso. *Journal of the Royal Statistical Society: Series B (Statistical Methodology)* **67** 91–108.
- VAN DE GEER, S. (2000). *Empirical Processes in M-Estimation*. Cambridge University Press.
- VAN DE GEER, S. and BUHLMANN, P. (2009). On the conditions used to prove oracle results for the Lasso. *Electronic Journal of Statistics* **3** 1360–1392.
- WANG, Y., SHARPNACK, J., SMOLA, A. and TIBSHIRANI, R. (2016). Trend filtering on graphs. *Journal of Machine Learning Research* **17** 1–41.
- WAUTHIER, F. L., JOJIC, N. and JORDAN, M. I. (2013). A Comparative Framework for Preconditioned Lasso Algorithms. In *Advances in Neural Information Processing Systems 26* (C. J. C. Burges, L. Bottou, M. Welling, Z. Ghahramani and K. Q. Weinberger, eds.) 1061–1069. Curran Associates, Inc.
- WITTEN, D., SHOJAIE, A. and ZHANG, F. (2014). The cluster elastic net for high-dimensional regression with unknown variable grouping. *Technometrics* **56** 112–122.
- WU, T. T., CHEN, Y. F., HASTIE, T., SOBEL, E. and LANGE, K. (2009). Genome-wide association analysis by lasso penalized logistic regression. *Bioinformatics* **25** 714–721.
- XIN, B., KAWAHARA, Y., WANG, Y. and GAO, W. (2014). Efficient Generalized Fused Lasso and its Application to the Diagnosis of Alzheimer’s Disease. In *AAAI* 2163–2169. Citeseer.
- XIN, B., KAWAHARA, Y., WANG, Y., HU, L. and GAO, W. (2016). Efficient generalized fused Lasso and its applications. *ACM Transactions on Intelligent Systems and Technology (TIST)* **7** 60.
- ZOU, H. (2006). The Adaptive Lasso and its Oracle Properties. *Journal of the American Statistical Association* **101** 1418–1429.
- ZOU, H. and HASTIE, T. (2005). Regularization and variable selection via the elastic net. *Journal of the Royal Statistical Society, Series B* **67(2)** 301–320.